Mean-Quadratic Variation Portfolio Optimization: A desirable alternative to Time-consistent Mean-Variance Optimization?

Pieter M. van Staden* Duy-Minh Dang† Peter A. Forsyth‡

October 24, 2018

Abstract

We investigate the Mean-Quadratic Variation (MQV) portfolio optimization problem and its relationship to the Time-consistent Mean-Variance (TCMV) portfolio optimization problem. In the case of jumps in the risky asset process and no investment constraints, we derive analytical solutions for the TCMV and MQV problems. We study conditions under which the two problems are (i) identical with respect to MV trade-offs, and (ii) equivalent, i.e. same value function and optimal control. We provide a rigorous and intuitive explanation of the abstract equivalence result between the TCMV and MQV problems developed in [T. Bjork and A. Murgoci, *Finance and Stochastics*, 18 (2014), pp. 545-592] for continuous rebalancing and no-jumps in risky asset processes. We extend this equivalence result to jump-diffusion processes (both discrete and continuous rebalancings).

In order to compare the MQV and TCMV problems in a more realistic setting which involves investment constraints and modelling assumptions for which analytical solutions are not known to exist, using a impulse control approach, we develop an efficient partial integro-differential equation (PIDE) method for determining the optimal control for the MQV problem. We also prove convergence of the proposed numerical method to the viscosity solution of the corresponding PIDE. We find that MQV investor achieves essentially the same results concerning terminal wealth as TCMV investor, but the MQV-optimal investment process has more desirable risk characteristics from the perspective of long-term investors with fixed investment time horizons. As a result, we conclude that MQV portfolio optimization is a potentially desirable alternative to the TCMV counterpart.

Keywords: Asset allocation, constrained optimal control, time-consistent, quadratic variation

JEL Subject Classification: G11, C61

1 Introduction

Mean-variance (MV) portfolio optimization is popular in modern portfolio theory due to the intuitive nature of the resulting investment strategies (Elton et al. (2014)). Two main approaches to perform MV portfolio optimization can be identified. The first approach, referred to as the pre-commitment MV approach, typically results in time-inconsistent optimal strategies (Basak and Chabakauri (2010); Bjork and Murgoci (2014); Vigna (2016)). This time-inconsistency phenomenon is due to the fact that the MV optimization problem fails to admit the Bellman optimality principle, since the variance term is not separable in the sense of dynamic programming (Li and Ng (2000); Zhou and Li (2000)).

The second approach to MV optimization, namely the Time-consistent MV (TCMV) or game theoretical approach, guarantees the time-consistency of the resulting optimal strategy by imposing

*School of Mathematics and Physics, The University of Queensland, St Lucia, Brisbane 4072, Australia, email: pieter.vanstaden@uq.edu.au

†School of Mathematics and Physics, The University of Queensland, St Lucia, Brisbane 4072, Australia, email: duyminh.dang@uq.edu.au

‡Cheriton School of Computer Science, University of Waterloo, Waterloo ON, Canada, N2L 3G1, paforsyt@uwaterloo.ca

a time-consistency constraint (Basak and Chabakauri (2010); Bjork and Murgoci (2014); Cong and Oosterlee (2016); Wang and Forsyth (2011)).[1] This means that TCMV problem can be solved using dynamic programming (Cong and Oosterlee (2016); Van Staden et al. (2018)).

The TCMV problem is referred to in Bjork et al. (2017); Bjork and Murgoci (2014) as "non-standard" problems, in that, without imposing the time-consistency constraint, the optimal control is time-inconsistent. It is further shown in Bjork et al. (2017); Bjork and Murgoci (2014) that, for every "non-standard" problem, there exists an equivalent "standard" optimal control problem which admits the Bellman optimality principle, so that the resulting optimal control is time-consistent without the need to impose a time-consistency constraint. Here, equivalence between two control problems is to be understood that they both have the same value function and optimal control.

In the case of the TCMV problem with continuous rebalancing, GBM dynamics for the risky asset process, and no investment constraints, Bjork and Murgoci (2010) shows that the equivalent standard problem to the TCMV problem, is in fact the mean-quadratic-variation (MQV) problem with a particular function of the quadratic variation (QV) of wealth being used as the risk measure.[2] From a numerical perspective, in the same setting, but with realistic investment constraints, Wang and Forsyth (2012) shows that both TCMV and MQV problems result in a very similar MV trade-off in the optimal terminal wealth. However, the two problems have quite different optimal controls, and hence, are not equivalent. These theoretical and numerical results suggest that a similarly deep relationship between the TCMV and MQV portfolio optimization may exist in a more general setting, such as discrete rebalancing, jumps in the risky asset processes and realistic investment constraints. However, to the best of our knowledge, a systematic and rigorous study of such relationship is not available in the literature.

While MQV optimization is popular in optimal trade execution (Almgren and Chriss, 2001; Forsyth et al., 2012; Tse et al., 2013), it is clearly not widely used in portfolio optimization settings. In particular, QV (or some function of QV) is not even widely used as a risk measure in portfolio optimization settings, and is usually not mentioned when popular risk measures are discussed (see for example McNeil et al. (2015), Elton et al. (2014), Rockafellar and Uryasev (2002)). This contrasts to the considerable popularity in the portfolio optimization literature enjoyed by the TCMV approach (see, for example, Alia et al. (2016); Bensoussan et al. (2014); Cui et al. (2015); Van Staden et al. (2018), among many other published works on TCMV). We argue that this is somewhat unfortunate, for reasons listed below.

- The MQV portfolio optimization problem retains many of the intuitive aspects of MV optimization, including the clear trade-off between risk and return.

- Measuring risk using the QV of the portfolio wealth over the investment period arguably offers the investor more control over the risk *throughout* the investment period, instead of just focusing on the risk *at* maturity, such as with the variance of terminal wealth. As a result, QV is of potential interest especially to institutional investors and portfolio managers who have to report regularly to stakeholders.

- Most importantly, from the perspective of this paper, a deep connection exists between TCMV and MQV portfolio optimization, and it can be exploited to the MV investor's advantage. For example, as shown in this paper, in a general setting with jumps in the risky asset and realistic investment constraints, a MQV strategy typically retains *all* of the terminal wealth characteristics of a TCMV strategy, but with a risky asset exposure profile over time that is arguably more suitable for long-term investors with a fixed investment time horizon.

[1] The time-consistency constraint should be distinguished from investment constraints, such as leverage or solvency constraints, which do not affect the time-consistency of the resulting optimal control.

[2] Quadratic variation of the (stochastic) portfolio value was first proposed as a risk measure in Brugiere (1996).

- Last but not least, the TCMV problem typically requires the solution of an extended Hamilton-Jacobi-Bellman (HJB) equation which falls outside the scope of viscosity solution theory of Crandall et al. (1992). Therefore, existing convergence results, e.g. Barles and Souganidis (1991), cannot be used to prove the convergence of a proposed PDE numerical scheme. By contrast, the MQV portfolio optimization problem does fall within the scope of viscosity solution theory of Crandall et al. (1992). This is a significant advantage of MQV over TCMV portfolio optimization, since if convergence can be proven, this will significantly increase the investor's confidence in the numerical results provided by the method

The main objective of this paper is to investigate the MQV portfolio optimization problem and its relationship to TCMV in a general setting, namely jumps in the risky asset processes, realistic investment constraints and modelling assumptions. This relationship is examined at two different levels, namely (i) MV trade-offs of terminal wealth, and (ii) equivalence, i.e. same value function and optimal control. In this work, we will not consider a wealth dependent risk aversion parameter, since it is shown in Van Staden et al. (2018) that the objective function in this case performs poorly for accumulation problems. We will focus on the constant risk aversion parameter case. Numerical methods for the TCMV problem are discussed in Van Staden et al. (2018).

The main contributions of this paper are as follows.

- We derive analytical solutions for the TCMV and MQV problems in the case of discrete rebalancing, jumps in the risky asset processes and no investment constraints. We show that, with a commonly used QV risk measure, the two problems result in identical MV trade-offs of terminal wealth, but with quite different investment strategies (controls), hence, not equivalent. Typically, the MQV-optimal strategy would consistently call for a higher investment in the risky asset. We then establish that, as the length of rebalancing intervals approaches zero (continuous rebalancing), the TCMV and MQV problems are indeed equivalent.

  We construct a QV risk measure which guarantees equivalence between the TCMV and MQV problems for both discrete and continuous rebalancings.

  These mathematical findings provide a rigorous and intuitive explanation of the abstract equivalence result between the TCMV and MQV problems developed in Bjork and Murgoci (2014) for the case of continuous rebalancing, with no jumps in the risky asset process and no investment constraints. Furthermore, these findings also extend the equivalence result of Bjork and Murgoci (2014) to the case of jumps in the risky asset process for both discrete and continuous rebalancings.

- We formulate the MQV portfolio optimization problem as a two-dimensional impulse control problem, with linear partial integro-differential equations (PIDEs) to be solved between intervention times. This approach allows for the simultaneous application of realistic investment constraints, including (i) discrete rebalancing, (ii) liquidation in the event of insolvency, (iii) leverage constraints, (iv) different interest rates for borrowing and lending, and (v) transaction costs. A convergence proof of the numerical PDE method to the viscosity solution of the associated quasi-integro-variational inequality is sketched. This highlights the above-mentioned theoretical advantage of MQV optimization relative to TCMV optimization, since the convergence of numerical methods to solve TCMV problems typically cannot be proven.

- We present a comprehensive comparison study of the MQV and TCMV optimization results, including characteristics of the resulting optimal investment strategies, terminal wealth distributions, mean-variance outcomes, and the effect of the simultaneous application of investment constraints. All numerical experiments are conducted using model parameters calibrated to inflation-adjusted, long-term US market data (89 years), enabling realistic conclusions to be drawn from the results.

We find that, while MQV and TCMV optimization give essentially identical terminal wealth outcomes even under realistic investment constraints, the MQV-optimal investment strategy calls for a significantly larger reduction in risky asset exposure as the investment maturity is approached. This provides further evidence in support of considering MQV optimization as a desirable alternative to TCMV portfolio optimization.

The remainder of the paper is organized as follows. Section 2 describes the underlying processes and modelling approach, including a description of TCMV and MQV portfolio optimization approaches. The relationship between TCMV and MQV optimization is analyzed in Section 3, and new analytical results are presented. In Section 4, a numerical method for solving the MQV problem is presented, along with a convergence proof of the proposed method. Numerical results are presented and discussed in Section 5. Finally, Section 6 concludes the paper and outlines possible future work.

2 Formulation

2.1 Underlying dynamics

Since we are concerned with investment problems with very long time horizons, we consider portfolios consisting of two assets only - a risky asset and a risk-free asset. For the risky asset, we consider a well-diversified index (see Section 5), instead of a single stock, which allows us to focus on the primary question of the stocks vs. bonds mix in the portfolio under different investment strategies, rather than secondary questions relating to risky asset basket compositions[3].

Let $S(t)$ and $B(t)$ denote the amounts respectively invested in the risky and risk-free asset at time $t \in [0, T]$, where $T > 0$ denotes the fixed investment time horizon/maturity. In the absence of control (when there is no intervention by the investor according to some control strategy), the dynamics of the amount $B(t)$ is assumed to be given by

$$dB(t) = \mathcal{R}(B(t))\, B(t)\, dt, \quad \text{where} \quad \mathcal{R}(B(t)) = r_\ell + (r_b - r_\ell)\, \mathbb{I}_{[B(t)<0]}, \tag{2.1}$$

where r_b and r_ℓ denote the positive, continuously compounded rates at which the investor can respectively borrow funds or earn on cash deposits (with $r_b > r_\ell$), while $\mathbb{I}_{[A]}$ denotes the indicator function of the event A.

Realistic modelling of $S(t)$ requires consideration of (i) jumps and (ii) stochastic volatility in the process dynamics. However, the results of Ma and Forsyth (2016) show that the effects of stochastic volatility, with realistic mean-reverting dynamics, are not important for long-term investors with time horizons greater than 10 years[4]. We therefore consider jump diffusion processes for the risky asset using a constant volatility parameter.

Let $t^- = \lim_{\epsilon \downarrow 0} (t - \epsilon)$ and $t^+ = \lim_{\epsilon \downarrow 0} (t + \epsilon)$. Informally, t^- (resp. t^+) denotes the instant of time immediately before (resp. after) the forward time t. Let ξ be a random variable denoting the jump multiplier, which has probability density function (pdf) $p(\xi)$. If a jump occurs at time t, the amount in the risky asset jumps from $S(t^-)$ to $S(t) = \xi S(t^-)$. We will consider two jump distributions of ξ. In the case of the Merton (1976) model, $\log \xi$ is normally distributed with mean $\widetilde{m}$ and standard deviation $\widetilde{\gamma}$, so that $p(\xi)$ is the log-normal pdf

$$p(\xi) \quad = \quad \frac{1}{\xi \sqrt{2\pi \widetilde{\gamma}^2}} \exp\left\{ -\frac{(\log \xi - \widetilde{m})^2}{2\widetilde{\gamma}^2} \right\}. \tag{2.2}$$

[3] In the available analytical solutions for multi-asset TCMV problems (see, for example, Zeng and Li (2011)) as well as pre-commitment MV problems (see for example Li and Ng (2000)), the composition of the risky asset basket remains relatively stable over time, which suggests that the primary question remains the overall risky asset basket vs. the risk-free asset composition of the portfolio, instead of the exact composition of the risky asset basket.

[4] While Ma and Forsyth (2016) considers the case of pre-commitment MV optimization, there is no reason to suspect the findings would be materially different for either TCMV or MQV optimization.

In the case of the Kou (2002) model, $\log \xi$ has an asymmetric double-exponential distribution, so that $p(\xi)$ is of the form

$$p(\xi) = \nu\zeta_1 \xi^{-\zeta_1-1} \mathbb{I}_{[\xi\geq 1]}(\xi) + (1-\nu)\zeta_2 \xi^{\zeta_2-1} \mathbb{I}_{[0\leq\xi<1]}(\xi), \quad \upsilon \in [0,1] \text{ and } \zeta_1 > 1, \zeta_2 > 0, \quad (2.3)$$

where ν denotes the probability of an upward jump (given that a jump occurs). For subsequent reference, we define $\kappa = \mathbb{E}[\xi - 1]$ and $\kappa_2 = \mathbb{E}\left[(\xi-1)^2\right]$. In the absence of control, the dynamics of the amount $S(t)$ is assumed to be given by

$$\frac{dS(t)}{S(t^-)} = (\mu - \lambda\kappa)\,dt + \sigma dZ + d\left(\sum_{i=1}^{\pi(t)} (\xi_i - 1)\right), \quad (2.4)$$

where μ and σ are the real world drift and volatility respectively, Z denotes a standard Brownian motion, $\pi(t)$ is a Poisson process with intensity $\lambda \geq 0$, and ξ_i are i.i.d. random variables with the same distribution as ξ. It is futhermore assumed that ξ_i, $\pi(t)$ and Z are mutually independent. Note that GBM dynamics for $S(t)$ can be recovered from (2.4) by setting the intensity parameter λ to zero.

Since we consider one risky asset, which has real world drift rate μ assumed to be strictly greater than r_ℓ, together with a constant parameter of risk aversion (see Subsections 2.4 and 2.5 below), it is neither MV-optimal nor MQV-optimal to short stock[5], so we consider only the case of $S(t) \geq 0$, $t \in [0,T]$. We do allow for short positions in the risk-free asset, i.e. it is possible that $B(t) < 0, t \in [0,T]$.

2.2 Portfolio rebalancing

Let $X(t) = (S(t), B(t))$, $t \in [0,T]$, denote the multi-dimensional controlled underlying process, and $x = (s,b)$ the state of the system. The liquidation value of the controlled portfolio wealth, possibly including transaction costs, is denoted by $W(t)$, where

$$W(t) = W(s,b) = b + \max\left[(1-c_2)s - c_1, 0\right], \qquad t \in [0,T]. \quad (2.5)$$

Here, $c_1 \geq 0$ and $c_2 \in [0,1)$ denotes the fixed and proportional transaction costs, respectively. Let $(\mathcal{F}_t)_{t\in[0,T]}$ be the natural filtration associated with the wealth process $\{W(t), t \in [0,T]\}$.

We use $\mathcal{C}_t$ to denote the control, representing an investment strategy as a function of the underlying state, computed at time $t \in [0,T]$, i.e. $\mathcal{C}_t(\cdot) : (X(t), t) \mapsto \mathcal{C}_t = \mathcal{C}(X(t), t)$, and applicable over the time interval $[t,T]$. An impulse control $\mathcal{C}_t$ is defined (Oksendal and Sulem (2005)) as the double, possibly finite, sequence

$$\mathcal{C}_t = (t_1, t_2, \ldots, t_n, \ldots;\ \eta_1, \eta_2, \ldots, \eta_n, \ldots)_{n\leq m} = (\{t_n, \eta_n\})_{1\leq n\leq m},\ m \leq \infty. \quad (2.6)$$

Here, the intervention times $(t_n)_{1\leq n\leq m}$ are any sequence of $(\mathcal{F}_t)$-stopping times satisfying the condition $t \leq t_1 < \ldots < t_m < T$, associated with a corresponding sequence of random variables $(\eta_n)_{1\leq n\leq m}$ denoting the impulse values, with each η_n being of $\mathcal{F}_{t_n}$-measurable for all t_n. We respectively denote by $\mathcal{Z}$ and $\mathcal{A}$ the sets of admissible impulse values and impulse controls, (defined in the next subsection).

In our application, each intervention time t_n corresponds to a rebalancing time of the portfolio, and the associated impulse η_n corresponds to the amount invested in the risk-free asset at this time (see (2.8) below). While the definition (2.6) allows for t_n to be *any* $(\mathcal{F}_t)$-stopping time, in practical settings we are of course limited to consider only a finite set of pre-specified potential intervention times, assumed to take the form of a uniform partition of the time interval $[0,T]$ denoted by $\mathcal{T}_m$, where

[5]For any finite time interval over which a position is held without rebalancing, the expected value of the QV of portfolio wealth would be the same for either a short initial position or an otherwise identical long initial position in the risky asset. A short position would therefore incur the same QV risk as an otherwise identical long position, but with less return (since $\mu > r_\ell$), and therefore cannot be MQV optimal.

$$\mathcal{T}_m \;=\; \{t_n |\, t_n = (n-1)\,\Delta t,\; n = 1, \ldots, m\}\,, \quad \Delta t = T/m. \tag{2.7}$$

We consider both "continuous rebalancing" and "discrete rebalancing" in this paper. By continuous rebalancing, we mean letting $\Delta t \downarrow 0$ (equivalently, $m \to \infty$) in (2.7), so that the investor recovers the ability to intervene according to definition (2.6).

Suppose that the investor considers applying impulse $\eta_n \in \mathcal{Z}$ at time $t_n \in \mathcal{T}_m$, and that the system is in state $x = (s, b)$ at time t_n^-. Letting $(S(t_n), B(t_n)) \equiv (S^+(s, b, \eta_n), B^+(s, b, \eta_n))$ denote the state of the system immediately after the application of the impulse η_n, we define

$$\begin{aligned} B(t_n) \equiv B^+(s, b, \eta_n) &= \eta_n, \\ S(t_n) \equiv S^+(s, b, \eta_n) &= (s + b) - \eta_n - c_1 - c_2 \cdot \left| S^+(s, b, \eta_n) - s \right|. \end{aligned} \tag{2.8}$$

Between any two intervention times, i.e. for $t \in \left[t_n^+, t_{n+1}^-\right]$, the amounts B and S evolve according to the dynamics specified in (2.1) and (2.4), respectively.

For simplicity, we introduce the following notational convention. Associated with a fixed set of intervention times $\mathcal{T}_m$ as in (2.7), an impulse $\mathcal{C} \in \mathcal{A}$ will be written as the set of impulses

$$\mathcal{C} \;=\; \{\eta_n \in \mathcal{Z} :\; n = 1, \ldots, m\}\,, \tag{2.9}$$

where the intervention times are implicitly understood to be the set $\mathcal{T}_m$. Given an impulse control $\mathcal{C}$ of the form (2.9), and an intervention time $t_n \in \mathcal{T}_m$, we define $\mathcal{C}_n$ to be the subset of impulses (and, implicitly, the corresponding intervention times) of $\mathcal{C}$ applicable to the time interval $[t_n, T]$:

$$\mathcal{C}_n \equiv \mathcal{C}_{t_n} = \{\eta_n, \eta_{n+1} \ldots, \eta_m\} \;\subseteq\; \mathcal{C} = \mathcal{C}_1 = \{\eta_1, \ldots, \eta_m\}\,. \tag{2.10}$$

2.3 Admissible portfolios

Fix an arbitrary intervention time $t_n \in \mathcal{T}_m$, and assume that the system is in state $x = (s, b) \in \Omega^\infty$ at time t_n^-, where $\Omega^\infty = [0, \infty) \times (-\infty, \infty)$ denotes the spatial domain. We consider enforcing a solvency constraint and a maximum leverage constraint as described below.

We define the solvency region $\mathcal{N}$ and the bankruptcy region $\mathcal{B}$ as follows:

$$\mathcal{N} \;=\; \{(s, b) \in \Omega^\infty :\; W(s, b) > 0\}\,, \tag{2.11}$$

$$\mathcal{B} \;=\; \{(s, b) \in \Omega^\infty :\; W(s, b) \le 0\}\,. \tag{2.12}$$

The solvency condition stipulates that if $W(s, b) \le 0$, i.e. $(s, b) \in \mathcal{B}$, then the position in the risky asset has to be liquidated, the total remaining wealth has to be placed in the debt accumulating at the borrowing rate, and all subsequent trading activities must cease. In other words,

$$\text{If } (s, b) \in \mathcal{B} \text{ at } t_n^- \;\Rightarrow\; \begin{cases} \text{we require } (S(t_n) = 0, B(t_n) = W(s, b)) \\ \text{and remains so } \forall t \in [t_n, T]\,. \end{cases} \tag{2.13}$$

The maximum leverage constraint is applied at each intervention time to ensure that the leverage ratio $\frac{S(t_n)}{S(t_n)+B(t_n)}$, where $(S(t_n), B(t_n))$ are computed by (2.8), satisfies

$$\frac{S(t_n)}{S(t_n) + B(t_n)} \;\le\; q_{\max}, \qquad n = 1, \ldots, m. \tag{2.14}$$

Here, $q_{\max}$ is typically in the range $q_{\max} \in [1.0, 2.0]$.

The set of admissible impulse values $\mathcal{Z}$ and admissible impulse controls $\mathcal{A}$ are defined as follows

$$\mathcal{Z} \;=\; \begin{cases} \left\{\eta \equiv B \in (-\infty, +\infty) : (S, B) \text{ via (2.8)}\right\} & \text{no constraints,} \\ \begin{cases} \left\{\eta \equiv B \in (-\infty, +\infty) : (S, B) \text{ via (2.8) s.t. } 0 \le S, \text{and } 0 \le \frac{S}{S+B} \le q_{\max}\right\} & (s, b) \in \mathcal{N} \\ \{\eta = W(s + b)\} & (s, b) \in \mathcal{B} \end{cases} & \text{solvency \& maximum leverage,} \end{cases}$$

$$\mathcal{A} \;=\; \left\{(\{\eta_n\})_{1 \le n \le m} : \eta_n \in \mathcal{Z}\right\}. \tag{2.15}$$

2.4 TCMV optimization

Let $E_{\mathcal{C}_n}^{x,t_n}[W(T)]$ and $Var_{\mathcal{C}_n}^{x,t_n}[W(T)]$ denote the mean and variance of terminal wealth, respectively, given state $x=(s,b)$ at time t_n^- (with $t_n \in \mathcal{T}_m$) and using impulse control $\mathcal{C}_n \in \mathcal{A}$ over $[t_n, T]$. The TCMV problem can be formulated as follows (Basak and Chabakauri, 2010; Bjork and Murgoci, 2014; Hu et al., 2012)

$$TCMV_{t_n}(\rho): \begin{cases} V^c(s,b,t_n) \coloneqq \sup\limits_{\mathcal{C}_n \in \mathcal{A}} \left(E_{\mathcal{C}_n}^{x,t_n}[W(T)] - \rho \cdot Var_{\mathcal{C}_n}^{x,t_n}[W(T)] \right), \quad \rho > 0, & (2.16) \\ \text{s.t. } \mathcal{C}_n = \left\{ \eta_n, \mathcal{C}_{n+1}^{c*} \right\} \coloneqq \left\{ \eta_n, \eta_{n+1}^{c*}, \ldots, \eta_m^{c*} \right\} \in \mathcal{A}, & (2.17) \\ \qquad \text{where } \mathcal{C}_{n+1}^{c*} \text{ is optimal for problem } \left(TCMV_{t_{n+1}}(\rho) \right). \end{cases}$$

The time-consistency constraint (2.17) ensures that the resulting TCMV optimal strategy $\mathcal{C}_n^{c*}$ is, in fact, time-consistent, so that dynamic programming can be applied directly to (2.16)-(2.17) to compute the associated optimal controls. The reader is referred to Van Staden et al. (2018) for a discussion of numerical solutions of problem $TCMV_{t_n}(\rho)$.

For subsequent use in the paper, we define the auxiliary function

$$U^c(s,b,t_n) \quad = \quad E_{\mathcal{C}_n^{c*}}^{x,t_n}[W(T)], \tag{2.18}$$

where $\mathcal{C}_n^{c*}$ is the TCMV-optimal control for (2.16)-(2.17). Using $U^c(\cdot)$, the $TCMV_{t_n}(\rho)$ problem defined in (2.16)-(2.17) can be written more compactly as

$$TCMV_{t_n}(\rho): \begin{cases} V^c(s,b,t_n) \coloneqq \sup\limits_{\eta_n \in \mathcal{Z}} J^c(\eta_n; s,b,t_n), \qquad \rho > 0, \quad \text{where} & (2.19) \\ J^c(\eta_n; s,b,t_n) = E_{\eta_n}^{x,t_n}\left[V^c(X_{n+1}, t_{n+1}) \right] - \rho \cdot Var_{\eta_n}^{x,t_n}\left[U^c(X_{n+1}, t_{n+1}) \right]. & (2.20) \end{cases}$$

Here, $X_{n+1} \coloneqq \left(S\left(t_{n+1}^-\right), B\left(t_{n+1}^-\right) \right)$, while the notation $E_{\eta_n}^{x,t_n}[\cdot]$ and $Var_{\eta_n}^{x,t_n}[\cdot]$ refer to the expectation and variance, respectively, using an arbitrary impulse $\eta_n \in \mathcal{Z}$ at time t_n together with the implied application of the optimal impulse control $\mathcal{C}_{n+1}^{c*}$ over the time interval $[t_{n+1}, T]$.

Given that the system is in state $x_0 = (s_0, b_0)$ at time $t = 0$, which corresponds to the first rebalancing time $t_1 \in \mathcal{T}_m$ (see (2.7)), for an arbitrary risk aversion parameter $\rho > 0$, we denote by $\mathcal{Y}_{\text{TCMV}(\rho)}$ the corresponding MV "efficient" portfolio. This set is defined by

$$\mathcal{Y}_{\text{TCMV}(\rho)} = \left\{ \left(\sqrt{Var_{\mathcal{C}^{c*}}^{x_0,t=0}[W(T)]},\ E_{\mathcal{C}^{c*}}^{x_0,t_1=0}[W(T)] \right) \right\}, \tag{2.21}$$

where $\mathcal{C}^{c*} = \mathcal{C}_1^{c*}$ solves the problem $(TCMV_{t_1}(\rho))$.

Definition 2.1. (TCMV efficient frontier) The TCMV efficient frontier, denoted by $\mathcal{Y}_{\text{TCMV}}$, is defined as $\mathcal{Y}_{\text{TCMV}} = \bigcup_{\rho>0} \mathcal{Y}_{\text{TCMV}(\rho)}$, where $\mathcal{Y}_{\text{TCMV}(\rho)}$ is defined in (2.21).

2.5 MQV optimization

For given state $x=(s,b)$ at time t_n^- (with $t_n \in \mathcal{T}_m$) and an admissible impulse control $\mathcal{C}_n \in \mathcal{A}$, we denote by $\Theta_{\mathcal{C}_n}^{x,t_n}$ the QV risk measure applicable to the time interval $[t_n, T]$. It is defined as follows (Tse et al. (2013); Wang and Forsyth (2012))

$$\Theta_{\mathcal{C}_n}^{x,t_n} \quad = \quad \sum_{k=n}^{m} \int_{t_k}^{t_{k+1}^-} e^{2\mathcal{R}(B(t))\cdot(T-t)} \cdot d\langle W \rangle_t, \tag{2.22}$$

$$\text{with } d\langle W \rangle_t \quad = \quad \sigma^2 S^2\left(t^-\right) dt + \int_0^\infty S^2\left(t^-\right)(\xi-1)^2 N(dt, d\xi), \tag{2.23}$$

where $\langle W \rangle$ denotes the QV of the controlled wealth process using impulse control $\mathcal{C}_n$, $N(dt, d\xi)$ denotes the Poisson random measure associated with the S-dynamics (Applebaum (2004)), and the

function $\mathcal{R}(B(t))$ is as defined in (2.1). Observe that definition (2.22) excludes the QV contributed by transaction costs at rebalancing times[6], otherwise the QV risk measure would inappropriately penalize an investment strategy for any trading, regardless of whether risky asset holdings are increased or decreased.

Given state $x = (s, b)$ at time t_n^-, we define the MQV value function problem as

$$MQV_{t_n}(\rho): \begin{cases} V^q(s,b,t_n) \coloneqq \sup\limits_{\mathcal{C}_n \in \mathcal{A}} \left(E_{\mathcal{C}_n}^{x,t_n} \left[W(T) - \rho \cdot \Theta_{\mathcal{C}_n}^{x,t_n} \right] \right), \quad \rho > 0, \\ \qquad \text{where } \Theta_{\mathcal{C}_n}^{x,t_n} \text{ defined by (2.22).} \end{cases} \tag{2.24}$$

We denote by $\mathcal{C}_n^{q*}$ the optimal impulse control of problem $MQV_{t_n}(\rho)$, and define the following auxiliary functions:

$$U^q(s,b,t_n) = E_{\mathcal{C}_n^{q*}}^{x,t_n}[W(T)], \qquad Q^q(s,b,t_n) = E_{\mathcal{C}_n^{q*}}^{x,t_n}\left[W^2(T)\right]. \tag{2.25}$$

The functions U^q and Q^q can be used to calculate the variance of terminal wealth under $\mathcal{C}_n^{q*}$ as

$$Var_{\mathcal{C}_n^{q*}}^{x,t_n}[W(T)] = Q^q(s,b,t_n) - \left(U^q(s,b,t_n)\right)^2, \tag{2.26}$$

which is useful for comparing the results from implementing MQV and TCMV investment strategies (see Definition 2.2 below). Furthermore, we follow Wang and Forsyth (2012) in defining

$$Qstd_{\mathcal{C}_n^{q*}}^{x,t_n}[W(T)] = \sqrt{E_{\mathcal{C}_n^{q*}}^{x,t_n}\left[\Theta_{\mathcal{C}_n^{q*}}^{x,t_n}\right]} = \sqrt{\frac{1}{\rho}\left[U^q(s,b,t_n) - V^q(s,b,t_n)\right]}, \tag{2.27}$$

which can be compared to the standard deviation of terminal wealth in certain situations (see for example Subsection 3 and Table 5.3 below).

Using an arbitrary impulse $\eta_n \in \mathcal{Z}$ at time t_n, followed by an application of the MQV-optimal impulse control $\mathcal{C}_{n+1}^{q*}$ over the time interval $[t_{n+1}, T]$, we define the following function,

$$J^q(\eta_n; s, b, t_n) = E_{\eta_n}^{x,t_n}\left[V^q(X_{n+1}, t_{n+1})\right] - \rho \cdot E_{\eta_n}^{x,t_n}\left[\int_{t_n}^{t_{n+1}^-} e^{2\mathcal{R}(B(t))\cdot(T-t)} \cdot d\langle W\rangle_t\right]. \tag{2.28}$$

Note that the function J^q corresponds to the objective function of the problem $MQV_{t_n}(\rho)$ in the particular case where controls of the form $\mathcal{C}_n = \left\{\eta_n \cup \mathcal{C}_{n+1}^{q*}\right\}$ are used in (2.24).

Given that the system is in state $x_0 = (s_0, b_0)$ at time $t = 0$, which corresponds to the first rebalancing time $t_1 \in \mathcal{T}_m$ (see (2.7)), for an arbitrary risk aversion parameter $\rho > 0$, we denote by $\mathcal{Y}_{\text{MQV}(\rho)}$ the following set

$$\mathcal{Y}_{\text{MQV}(\rho)} = \left\{ \left(\sqrt{Var_{\mathcal{C}^{q*}}^{x_0,t=0}[W(T)]},\ E_{\mathcal{C}^{q*}}^{x_0,t_1=0}[W(T)] \right) \right\}, \tag{2.29}$$

where $Var_{\mathcal{C}^{q*}}^{x_0,t=0}[W(T)]$ is defined in (2.26), and $\mathcal{C}^{q*} = \mathcal{C}_1^{q*}$ solves the problem (2.24). We have the following definition.

Definition 2.2. (MQV frontier) The MQV frontier $\mathcal{Y}_{\text{MQV}}$ is defined as follows $\mathcal{Y}_{\text{MQV}} = \bigcup_{\rho>0} \mathcal{Y}_{\text{MQV}(\rho)}$, where $\mathcal{Y}_{\text{MQV}(\rho)}$ is defined in (2.29).

We note that, while the definition of the MQV frontier $\mathcal{Y}_{\text{MQV}}$ enables the like-for-like comparison with the TCMV efficient frontier $\mathcal{Y}_{\text{TCMV}}$ (Definition 2.1), MQV-optimal portfolios are not designed to be "MV efficient", since the variance of terminal wealth does not form part of the objective function of the MQV problem. In this paper, we therefore use the term MV *efficient* frontier exclusively for $\mathcal{Y}_{\text{TCMV}}$, and refer to $\mathcal{Y}_{\text{MQV}}$ as simply the MQV frontier, without reference to MV efficiency.

[6] If transaction costs are zero ($c_1 = c_2 = 0$ in (2.8)), the wealth of a self-financing portfolio remains unchanged through a rebalancing event.

3 Relationship between problems $TCMV_{t_n}(\rho)$ and $MQV_{t_n}(\rho)$

In this section, the theoretical aspects of the relationship between the TCMV and MQV problems are investigated in detail. To enable a meaningful comparison, the same investment constraints, modeling assumptions, and model parameters are applied to both problems. For subsequent reference, we introduce the following definitions.

Definition 3.1. (Identical frontiers) The TCMV and MQV problems are defined to have *identical frontiers* if $\mathcal{Y}_{\text{TCMV}} = \mathcal{Y}_{\text{MQV}}$, where $\mathcal{Y}_{\text{TCMV}}$ and $\mathcal{Y}_{\text{MQV}}$ are respectively defined in Definition 2.1 and Definition 2.2. That is, $\forall(\mathcal{V},\mathcal{E}) \in \mathcal{Y}_{\text{TCMV}}$, $\exists \rho^{'} > 0$ such that $(\mathcal{V},\mathcal{E}) = \mathcal{Y}_{\text{MQV}(\rho')}$, and vice versa.

We note that identical frontiers would imply that the two problems result in an identical MV trade-off in the optimal terminal wealth.

Definition 3.2. (Equivalence) Problems $TCMV_{t_n}(\rho)$ defined in (2.16) - (2.17) and $MQV_{t_n}(\rho)$ defined in (2.24) are equivalent if, for any fixed value of $\rho > 0$, they result in (i) the same optimal investment strategy or control, i.e. $\mathcal{C}_n^{q*} = \mathcal{C}_n^{c*}$, and (ii) the same value function, i.e. $V^q(s,b,t_n) = V^c(s,b,t_n)$, for all $n = 1,\ldots,m$ and all $x = (s,b)$.

Remark 3.3. (Equivalence and identical frontiers) If the TCMV and MQV problems are equivalent according to Definition 3.2, then, necessarily, they also have identical frontiers (Definition 3.1). Conversely, if the frontiers are not identical, then the problems cannot be equivalent. However, identical frontiers do not necessarily imply equivalence of the underlying problems, only that the same relationship holds between the mean and variance of the terminal wealth under the respective optimal strategies.

We first investigate the two problems in the case of discrete rebalancing. We assume a fixed, given set $\mathcal{T}_m$ of equally spaced rebalancing times as in (2.7), where Δt can remain non-infinitesimal.

Assumption 3.1. *Lending and borrowing rates are equal to the risk-free rate ($r_\ell = r_b = r$), and transaction costs are zero ($c_1 = c_2 = 0$). Trading continues in the event of insolvency, and no leverage constraint is applicable, i.e. $\mathcal{Z}$ is given by* (2.15).

The analytical solution of problems $TCMV_{t_n}(\rho)$ and $MQV_{t_n}(\rho)$ in the case of discrete rebalancing of the portfolio are given by the following lemmas.

Lemma 3.4. *(Analytical solution: TCMV problem with discrete rebalancing). If the system is in state $x = (s,b)$ at time t_n^-, where $t_n \in \mathcal{T}_m$, $n \in \{1,\ldots,m\}$, then in the case of discrete rebalancing under Assumption 3.1, the value function of problem $TCMV_{t_n}(\rho)$ in (2.16) is given by*

$$V^c(s,b,t_n) = U^c(s,b,t_n) - \rho(T-t_n)\left(\frac{1}{2\rho}K^c\right)^2 \cdot \frac{1}{\Delta t}\left(e^{\left(2\mu+\sigma^2+\lambda\kappa_2\right)\Delta t} - e^{2\mu\Delta t}\right), \tag{3.1}$$

where constant K^c, auxiliary function U^c (see (2.18)), and TCMV optimal impulse are respectively given by

$$K^c = \frac{\left(e^{\mu\Delta t} - e^{r\Delta t}\right)}{\left(e^{(2\mu+\sigma^2+\lambda\kappa_2)\Delta t} - e^{2\mu\Delta t}\right)}, \tag{3.2}$$

$$U^c(s,b,t_n) = (s+b)\,e^{r(T-t_n)} + (T-t_n)\left(\frac{1}{2\rho}K^c\right)\frac{1}{\Delta t}\left(e^{\mu\Delta t} - e^{r\Delta t}\right), \tag{3.3}$$

$$\eta_n^{c*} = s + b - \left(\frac{1}{2\rho}K^c\right)e^{-r(T-t_n)}e^{r\Delta t}. \tag{3.4}$$

Proof. See Appendix A. □

Lemma 3.5. *(Analytical solution: MQV problem with discrete rebalancing). If the system is in state $x = (s, b)$ at time t_n^-, where $t_n \in \mathcal{T}_m$, $n \in \{1, \ldots, m\}$, then in the case of discrete rebalancing under Assumption 3.1, the value function of problem $MQV_{t_n}(\rho)$ in (2.24) is given by*

$$V^q(s, b, t_n) = (s+b)\, e^{r(T-t_n)} + \frac{1}{2}(T-t_n)\left(\frac{1}{2\rho}K^q\right)\left(e^{\mu\Delta t} - e^{r\Delta t}\right)\frac{1}{\Delta t}e^{-2r\Delta t}, \tag{3.5}$$

where the constant K^q, auxiliary functions U^q and Q^q (see (2.25)), and the MQV-optimal impulse are respectively given by

$$K^q = \frac{\left(2\mu - 2r + \sigma^2 + \lambda\kappa_2\right)}{(\sigma^2 + \lambda\kappa_2)}\frac{\left(e^{\mu\Delta t} - e^{r\Delta t}\right)}{\left(e^{(2\mu-2r+\sigma^2+\lambda\kappa_2)\Delta t} - 1\right)}, \tag{3.6}$$

$$U^q(s, b, t_n) = (s+b)\, e^{r(T-t_n)} + (T-t_n)\left(\frac{1}{2\rho}K^q\right)\left(e^{\mu\Delta t} - e^{r\Delta t}\right)\frac{1}{\Delta t}e^{-2r\Delta t}, \tag{3.7}$$

$$Q^q(s, b, t_n) = \left(U^q(s, b, t_n)\right)^2 + (T-t_n)\left(\frac{1}{2\rho}K^q\right)^2\left(e^{\left(2\mu+\sigma^2+\lambda\kappa_2\right)\Delta t} - e^{2\mu\Delta t}\right)\frac{1}{\Delta t}e^{-4r\Delta t}, \tag{3.8}$$

$$\eta_n^{q*} = s + b - \left(\frac{1}{2\rho}K^q\right)e^{-r(T-t_n)}e^{-r\Delta t}. \tag{3.9}$$

Proof. See Appendix A. □

3.1 Identical frontiers ($\mathcal{Y}_{\text{TCMV}} = \mathcal{Y}_{\text{MQV}}$)

The results from Lemma 3.4 and Lemma 3.5 are used to derive an important relationship between the TCMV and MQV problems, given in the next theorem.

Theorem 3.6. *($\mathcal{Y}_{TCMV} = \mathcal{Y}_{MQV}$). In the case of discrete rebalancing under Assumption 3.1, we have $\mathcal{Y}_{TCMV} = \mathcal{Y}_{MQV}$ (Definition 3.1). Specifically, given $x_0 = (s_0, b_0)$ at time $t = t_1 = 0$, with initial wealth $w_0 = s_0 + b_0$, both $\mathcal{Y}_{TCMV}$ and $\mathcal{Y}_{MQV}$ coincide with a line with intercept $w_0 e^{rT}$ and slope M_f, where*

$$M_f = \frac{\left(e^{\mu\Delta t} - e^{r\Delta t}\right)}{\sqrt{\left(e^{(2\mu+\sigma^2+\lambda\kappa_2)\Delta t} - e^{2\mu\Delta t}\right)}} \cdot \sqrt{\frac{T}{\Delta t}}. \tag{3.10}$$

Proof. Combining (3.1) and (3.3) (resp. combining (3.7) and (3.8) with (2.26)), the TCMV-optimal (resp. MQV-optimal) standard deviation of terminal wealth is given by

$$Stdev_{\mathcal{C}^{c*}}^{x_0,t=0}[W(T)] = \left(\frac{1}{2\rho}K^c\right)\cdot\sqrt{\frac{T}{\Delta t}\left(e^{(2\mu+\sigma^2+\lambda\kappa_2)\Delta t} - e^{2\mu\Delta t}\right)}, \tag{3.11}$$

$$Stdev_{\mathcal{C}^{q*}}^{x_0,t=0}[W(T)] = \left(\frac{1}{2\rho}K^q\right)e^{-2r\Delta t}\sqrt{\frac{T}{\Delta t}\left(e^{(2\mu+\sigma^2+\lambda\kappa_2)\Delta t} - e^{2\mu\Delta t}\right)}. \tag{3.12}$$

Evaluating (3.3) at $(s, b, t_n) = (s_0, b_0, t = 0)$, substituting (3.11) and rearranging the result gives $\mathcal{Y}_{\text{TCMV}}$. The same steps with (3.12) and (3.7) results in $\mathcal{Y}_{\text{MQV}}$. In both cases, using $\mathcal{C}^*$ to denote either the TCMV optimal control or the MQV optimal control, we obtain

$$E_{\mathcal{C}^*}^{t=0}[W(T)] = w_0 e^{rT} + M_f \cdot \left(Stdev_{\mathcal{C}^*}^{t=0}[W(T)]\right). \tag{3.13}$$

□

The results of Theorem 3.6 show that, in a realistic setting of jumps in the risky asset process and discrete portfolio rebalancing, an MV investor who is only concerned with the MV trade-off of optimal terminal wealth would therefore be indifferent as to whether TCMV or MQV optimization is performed. However, as discussed in Remark 3.3, Theorem 3.6 does *not* imply the equivalence of problems $TCMV_{t_n}(\rho)$ and $MQV_{t_n}(\rho)$ in the sense of Definition 3.2.

As an illustration, in Figure 3.1, we plot, for different ρ values, the expected values and standard deviations of optimal terminal wealth for the TCMV and MQV problems obtained with a particular set of parameters. It is clear that for any fixed value of ρ, the MQV strategy achieves both a higher expected value *and* a higher standard deviation of terminal wealth compared to the corresponding TCMV strategy. That is, $E_{\mathcal{C}_1^{c*}}^{x,t_1}[W(T)] < E_{\mathcal{C}_1^{q*}}^{x,t_1}[W(T)]$ and $Var_{\mathcal{C}_1^{c*}}^{x,t_1}[W(T)] < Var_{\mathcal{C}_1^{q*}}^{x,t_1}[W(T)]$.

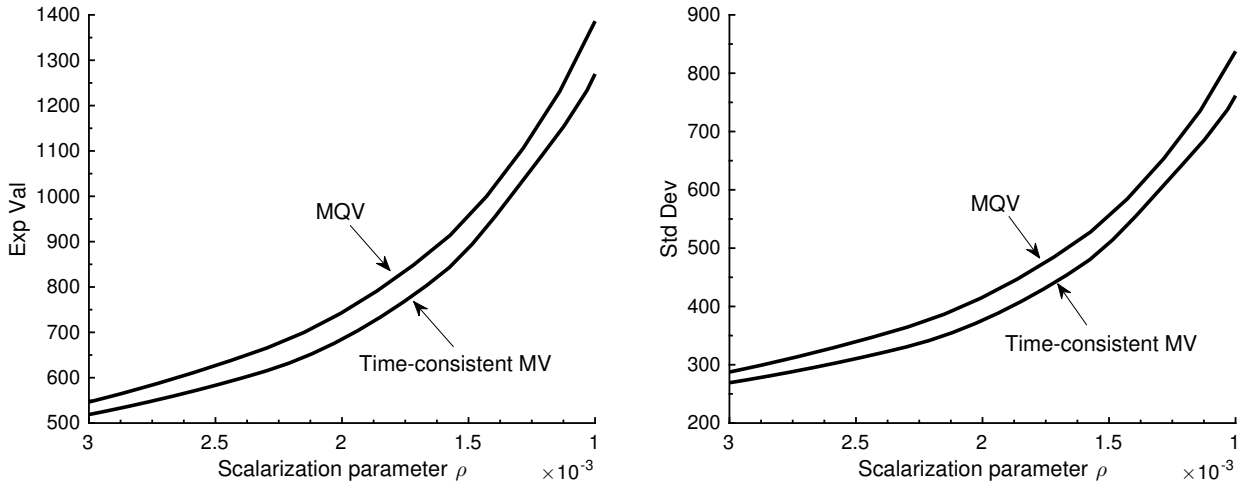

(a) Expected value of $W(T)$ vs. ρ

(b) Standard deviation of $W(T)$ vs. ρ

Figure 3.1: Expected value and standard deviation of optimal terminal wealth as a function of the scalarization parameter ρ. Discrete rebalancing ($\Delta t = 1$ year) under the conditions of Assumption 3.1, $T = 20$ years, and Kou model with parameters in Table 5.1.

Since the resulting optimal strategies/controls depend on the parameterization of the underlying process dynamics, we cannot make completely general conclusions as to how the TCMV-optimal and MQV-optimal controls are related. However, in typical applications where the risky asset represents a well-diversified stock index, and the risk-free rate is based on inflation-adjusted US government bond data (see for example the parameters in Dang and Forsyth (2016); Forsyth and Vetzal (2017) as well as Table 5.1 below), the conditions of the following theorem are satisfied, explaining that the results observed in Figure 3.1 are to be expected.

Theorem 3.7. *(Comparison of the TCMV and MQV optimal controls) Consider the case of discrete rebalancing under Assumption 3.1, with a fixed rebalancing time interval $\Delta t > 0$, with $\Delta t \sim \mathcal{O}(1)$. Suppose that the parameters of the underlying asset dynamics (2.1)-(2.4) satisfy $0 < r \ll \mu \ll 1$ and $\left(\sigma^2 + \lambda\kappa_2\right) \ll 1$. Then, for any fixed $\rho > 0$, we have that $\eta_n^{c*} > \eta_n^{q*}$, $n = 1, \ldots, m$, where η_n^{c*} and η_n^{q*} respectively are optimal impulse control for $TCMV_{t=0}(\rho)$ and $MQV_{t=0}(\rho)$ at intervention time t_n.*

Proof. The difference between the TCMV-optimal investment (3.4) and the MQV-optimal investment (3.9) in the *risk-free* asset at an arbitrary rebalancing time $t_n \in \mathcal{T}_m$ is given by

$$\eta_n^{c*} - \eta_n^{q*} = \frac{1}{2\rho} e^{-r(T-t_n)} e^{r\Delta t} \cdot \left(K^q e^{-2r\Delta t} - K^c\right). \tag{3.14}$$

Define the function $\varphi(\Delta t) = \left(e^{2\mu\Delta t} - e^{2r\Delta t}\right) / \left(e^{\left(2\mu+\sigma^2+\lambda\kappa_2\right)\Delta t} - e^{2\mu\Delta t}\right)$. Re-arranging (3.14), it is the case that $\left(\eta_n^{c*} - \eta_n^{q*}\right) > 0$ if

$$\varphi(\Delta t) < \frac{2(\mu - r)}{(\sigma^2 + \lambda\kappa_2)}, \text{ for all } \Delta t > 0. \tag{3.15}$$

Under the stated conditions on the parameters of the underlying dynamics, the derivative of $\varphi(\Delta t)$ is negative, so that the limit $\lim_{\Delta t \downarrow 0} \varphi(\Delta t) = 2(\mu - r) / \left(\sigma^2 + \lambda\kappa_2\right)$ is approached from below as $\Delta t \downarrow 0$. As a result, (3.15) holds, and the conclusion of the theorem follows. □

We argue that the conclusion of Theorem 3.7 is not necessarily a concern for MV investors. This is because, in practice, instead of making an abstract choice for a particular value of ρ, a MV investor is much more likely to make a concrete choice, such as a target expectation or variance of terminal wealth. In this case, the investor would be indifferent as to whether TCMV or MQV objective is used.

3.2 Equivalence between $TCMV_{t_n}(\rho)$ and $MQV_{t_n}(\rho)$

We now study the equivalence between the TCMV and MQV problems. The following lemma confirms that the difference between the TCMV and MQV optimal controls vanishes in the limit as $\Delta t \downarrow 0$. That is, in the case of continuous rebalancing, the two problems are equivalent as per Definition 3.2.

Theorem 3.8. *(Equivalence of problems $TCMV_{t_n}(\rho)$ and $MQV_{t_n}(\rho)$ - continuous rebalancing). Fix a value of the $\rho > 0$, and assume state $x = (s, b)$ at time t_n^-. In the case of continuous rebalancing ($\Delta t \downarrow 0$), for both the TCMV and MQV problems, the optimal control at any rebalancing time $t_n \in [0, T]$ is given by*

$$\eta_n^* = s + b - \frac{(\mu - r)}{2\rho\left(\sigma^2 + \lambda\kappa_2\right)} e^{-r(T-t_n)}. \tag{3.16}$$

Furthermore, the mean and standard deviation of optimal terminal wealth at time $t = 0$ (with initial wealth w_0) are respectively given by

$$E_{\mathcal{C}^*}^{t=0}\left[W(T)\right] = w_0 e^{rT} + \left(\frac{\mu - r}{\sqrt{\sigma^2 + \lambda\kappa_2}}\right)\sqrt{T} \cdot \left(Stdev_{\mathcal{C}_0^*}^{t=0}\left[W(T)\right]\right), \tag{3.17}$$

$$Stdev_{\mathcal{C}^*}^{t=0}\left[W(T)\right] = \frac{1}{2\rho}\left(\frac{\mu - r}{\sqrt{\sigma^2 + \lambda\kappa_2}}\right)\sqrt{T}. \tag{3.18}$$

Proof. The result follows from taking limits in the results presented in Lemma 3.4, Lemma 3.5 and Theorem 3.6, observing that $\lim_{\Delta t \downarrow 0} K^q = \lim_{\Delta t \downarrow 0} K^c = (\mu - r) / \left(\sigma^2 + \lambda\kappa_2\right)$. □

We now highlight the significance of Theorem 3.8. Firstly, by setting the jump intensity λ to zero, this theorem provides a rigorous and intuitive explanation of the abstract equivalence result between the TCMV and MQV problems developed in Bjork and Murgoci (2014) in the case of continuous rebalancing and no jumps in the risky asset process. Furthermore, with $\lambda > 0$, Theorem 3.8 extends the above-mentioned equivalence result of Bjork and Murgoci (2014) to the case of jumps in the risky asset process (still continuous rebalancing). Finally, this theorem also recovers the known analytical solutions of the optimal control (3.16), expectation and standard deviation of optimal terminal wealth (3.17)-(3.18) for the TCMV problem developed in Basak and Chabakauri (2010); Zeng et al. (2013). for the case of continuous rebalancing.

In the case of discrete rebalancing, the question of equivalence in the sense of Definition 3.2 remains. We now show that it is possible to construct a QV risk measure which guarantees equivalence between the TCMV problem and MQV problem using this risk measure in both discrete and continuous rebalancings. Given some state $x = (s, b)$ at time t_n^- with $t_n \in \mathcal{T}_m$, we define the *adjusted* Mean-Quadratic Variation (aMQV) problem using an adjusted QV risk measure $\widehat{\Theta}_{\mathcal{C}_n}^{x,t_n}$ as

$$aMQV_{t_n}(\rho): \begin{cases} \hat{V}^q(x, t_n) = \sup\limits_{\mathcal{C}_n \in \mathcal{A}} \left(E_{\mathcal{C}_n}^{x,t_n}\left[W(T) - \rho\widehat{\Theta}_{\mathcal{C}_n}^{x,t_n}\right]\right), \quad \rho > 0, \quad \text{where} & (3.19) \\ \widehat{\Theta}_{\mathcal{C}_n}^{x,t_n} = \int_{t_n}^{T} f(t)\, d\langle W\rangle_t, & (3.20) \\ f(t) = \sum\limits_{k=1}^{m} f_k(t)\, \mathbb{I}_{[t_k, t_{k+1})}(t), \quad t \in [0, T], & (3.21) \\ f_k(t) = e^{2r(T-t)}\left(1 + \frac{2(\mu - r)}{(\sigma^2 + \lambda\kappa_2)}\left[1 - e^{-\left(\sigma^2 + \lambda\kappa_2\right)(t - t_k)}\right]\right). & (3.22) \end{cases}$$

We observe that the adjusted QV risk measure (3.20) is a generalization of the QV risk measure (2.22) considered up to this point[7]. Figure 3.2 illustrates some key properties of the non-negative function of time $f : [0, T] \to [0, \infty)$, namely: (i) in the limit as $\Delta t \downarrow 0$ (i.e. continuous rebalancing) with zero transaction costs, the original QV risk measure (2.22) is recovered, and (ii) $f(t) \geq e^{2r(T-t)}, t \in [0, T]$ which implies that for any fixed $\rho > 0$, the QV risk calculated using the adjusted QV risk measure would be higher compared to the original QV risk. This should reduce the investment in the risky asset for problem $aMQV_{t_n}(\rho)$ compared to problem $MQV_{t_n}(\rho)$ for the same ρ value. This is a desirable outcome, given the conclusion of Theorem 3.7.

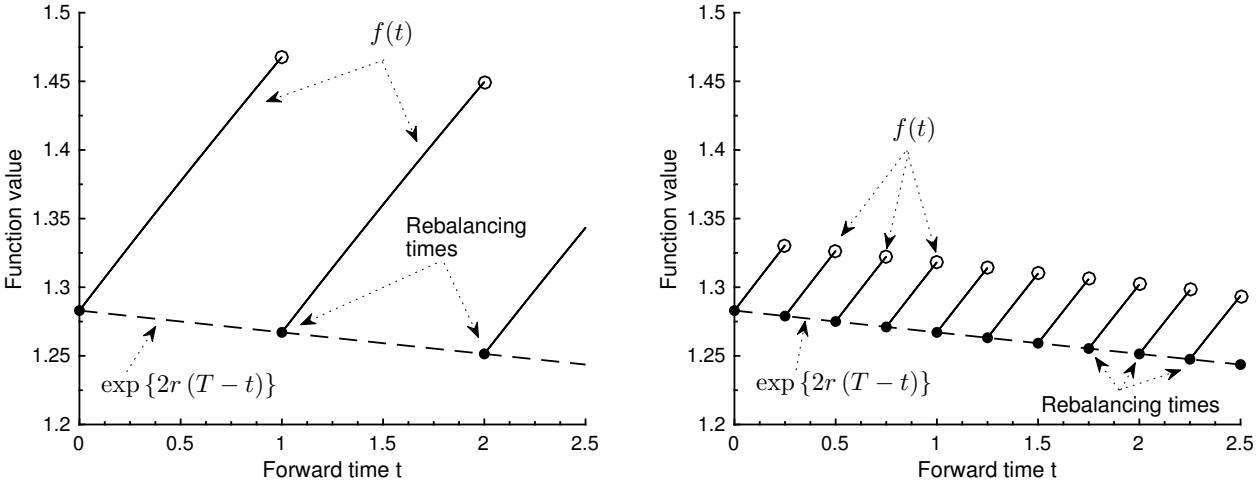

(a) Annual rebalancing

(b) Quarterly rebalancing

Figure 3.2: Function $f(t)$ defined in (3.21)-(3.22) compared to $e^{2r(T-t)}$ over $t \in [0, 2.5]$, with $T = 20$ years (Kou model, parameters as in Table 5.1). Note the same scale on the y-axis.

Theorem 3.9. *(Equivalence of problems $TCMV_{t_n}(\rho)$ and $aMQV_{t_n}(\rho)$ - discrete rebalancing) In the case of discrete rebalancing under Assumption 3.1, the TCMV problem $TCMV_{t_n}(\rho)$ and the adjusted MQV problem $aMQV_{t_n}(\rho)$ defined by (3.19)-(3.22) are equivalent in the sense of Definition 3.2.*

Proof. The proof relies on backward induction, using similar arguments as in Appendix A, therefore only a brief summary is given below. At time $t_{m+1} = T$, the value functions of problems $TCMV_{t_{m+1}}(\rho)$ and $aMQV_{t_{m+1}}(\rho)$ are trivially equal. Fix a value of $\rho > 0$, and an arbitrary rebalancing time $t_n \in \mathcal{T}_m$, with a given state $x = (s, b)$ at t_n^-, and assume that the value functions of problems $TCMV_{t_{n+1}}(\rho)$ and $aMQV_{t_{n+1}}(\rho)$ are equal. The objective functional of $TCMV_{t_n}(\rho)$ satisfies the recursive relationship (2.20), and since Assumption 3.1 is satisfied, the auxiliary function U^c is given by (3.3). If f_n is given by (3.22), we obtain the relationship

$$Var_{\eta_n}^{x,t_n}\left[U^c\left(S\left(t_{n+1}^-\right), B\left(t_{n+1}^-\right), t_{n+1}\right)\right] = E_{\eta_n}^{x,t_n}\left[\int_{t_n}^{t_{n+1}^-} f_n(t)\, d\langle W\rangle_t\right], \quad n = 1, \ldots, m, \tag{3.23}$$

which implies that the objective functionals of problems $TCMV_{t_n}(\rho)$ and $aMQV_{t_n}(\rho)$ are equal, and the conclusions follow. □

The significance of Theorem 3.9 is that it extends the TCMV-MQV equivalence result of Bjork and Murgoci (2010) from (i) continuous rebalancing and without jumps in the risky asset process to (ii) discrete rebalancing and with jumps in the risky asset process. Furthermore, if a TCMV investor is concerned about switching to using a MQV objective, since the optimal investment strategies may

[7] In the case of $r_\ell = r_b = r$ and zero transaction costs, this can be seen by rewriting the definition of the original QV risk measure (2.22) as $\Theta_{\mathcal{C}_n}^{x,t_n} = \int_{t_n}^{T}\left(\sum_{k=n}^{m} e^{2r(T-t)}\mathbb{I}_{[t_k,t_{k+1})}(t)\right)\cdot d\langle W\rangle_t$.

differ for a fixed value of ρ (Theorem 3.7), switching to an adjusted MQV objective (3.19) eliminates this concern entirely.

Although all the preceding results were proven under the conditions of Assumption 3.1, the results are also of great assistance when explaining the close correspondence between TCMV and MQV investment outcomes when multiple realistic investment constraints are applied (see Section 5). For example, we find that the resulting MV frontiers remain almost identical regardless of investment constraints, so that the main qualitative conclusion of Theorem 3.6 holds even when its conditions are violated.

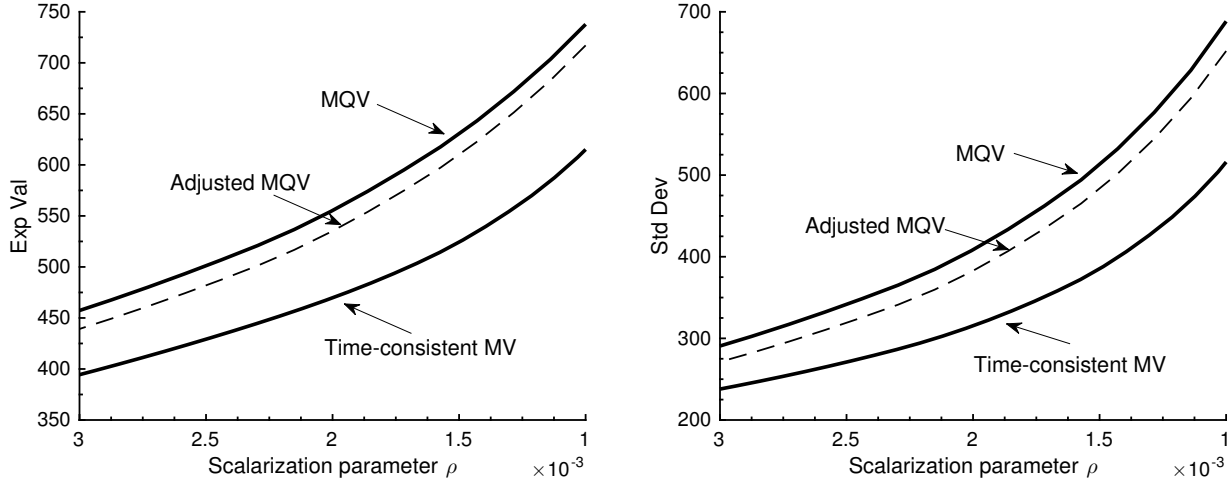

(a) Expected value of $W(T)$ vs. ρ

(b) Standard deviation of $W(T)$ vs. ρ

Figure 3.3: Mean and standard deviation of optimal terminal wealth as a function of ρ, subject to more realistic investment constraints (liquidation in the event of bankruptcy, maximum leverage ratio $q_{\max} = 1.5$). Kou model, parameters as in Table 5.1, $T = 20$ years, annual rebalancing.

Of course, there is no reason to expect that problems $TCMV_{t_n}(\rho)$ and $aMQV_{t_n}(\rho)$ should be equivalent (according to Definition 3.2) when realistic investment constraints are applied, and Figure 3.3 shows that this is indeed the case[8], although the results of problem $aMQV_{t_n}(\rho)$ seem to be slightly closer to problem $TCMV_{t_n}(\rho)$, as expected. However, in experimental results we found no discernible difference between the MV frontiers and terminal wealth distribution characteristics obtained from the MQV and adjusted MQV problems in the presence of investment constraints. All subsequent results in this paper are therefore formulated and presented in terms of the problem $MQV_{t_n}(\rho)$, with the construction of more general adjusted QV risk measures being left for our future work.

4 Numerical methods for MQV optimization

In seeking analytical solutions to the TCMV and MQV problems (see Section 3), we are typically severely limited in terms of the realistic investment constraints that can be applied, especially when multiple constraints are to be applied simultaneously - see for example Van Staden et al. (2018) for a discussion regarding the TCMV problem. For the purposes of a comprehensive comparison study of the MQV and TCMV investment outcomes, we therefore have to solve the MQV problem numerically to allow for the simultaneous application of multiple realistic investment constraints, including (i) the discrete rebalancing of the portfolio, (ii) liquidation in the event of insolvency, (iii) leverage constraints, (iv) different interest rates for borrowing and lending, and (v) transaction costs.

With this objective in mind, we develop an efficient numerical method for solving the MQV value function problem (2.24). We focus initially on the case of continuous rebalancing which, in a discretized

[8]The MQV and adjusted MQV results in Figure 3.3 were obtained using the algorithm developed in Section 4.

setting, means that the portfolio is rebalanced at every timestep (see Subsection 2.2). The case of discrete rebalancing is handled by making only a few small adjustments to the proposed numerical method, as discussed Remark 4.4.

Define $\tau = T - t$, $V(s,b,\tau) = V^q(s,b,T-t)$, as well as the following operators:

$$\mathcal{L}f(s,b,\tau) = (\mu - \lambda\kappa) sf_s + \mathcal{R}(b) bf_b + \frac{1}{2}\sigma^2 s^2 f_{ss} - \lambda f, \tag{4.1}$$

$$\mathcal{P}f(s,b,\tau) = (\mu - \lambda\kappa) sf_s + \frac{1}{2}\sigma^2 s^2 f_{ss} - \lambda f, \tag{4.2}$$

$$\mathcal{J}f(s,b,\tau) = \lambda \int_0^\infty f(\xi s, b, \tau) p(\xi) d\xi, \tag{4.3}$$

$$\mathcal{M}f(s,b,\tau) = \sup_{\eta \in \mathcal{Z}} \left[f\left(S^+(s,b,\eta), B^+(s,b,\eta), \tau\right)\right], \tag{4.4}$$

where f is an appropriate test function, and the values of $S^+(\cdot)$ and $B^+(\cdot)$ in the definition of the intervention operator[9] (4.4) is calculated according to (2.8). Using standard arguments (see Oksendal and Sulem (2005)), the value function $V(s,b,\tau)$ of problem $MQV_\tau(\rho)$ can be shown to satisfy the following quasi-integrovariational inquality in domain $(s,b,\tau) \in \Omega^\infty \times [0,T]$:

$$\begin{aligned}
\min\left\{V_\tau - \mathcal{L}V - \mathcal{J}V + \rho\left(\sigma^2 + \lambda\kappa_2\right) e^{2\mathcal{R}(b)\tau} s^2,\ V - \mathcal{M}V\right\} &= 0, \quad \text{if } (s,b,\tau) \in \mathcal{N} \times (0,T], \\
\min\left\{V_\tau - \mathcal{R}(b) bV_b,\ V - \mathcal{M}V\right\} &= 0, \quad \text{if } s = 0, \\
V(s,b,\tau) - V(0, W(s,b), \tau) &= 0, \quad \text{if } (s,b,\tau) \in \mathcal{B} \times (0,T], \\
V(s,b,0) - W(s,b) &= 0, \quad \text{if } \tau = 0.
\end{aligned} \tag{4.5}$$

4.1 Localization

For computational purposes, we localize the domain of (4.5), $\Omega^\infty \times [0,T] = [0,\infty) \times (-\infty,\infty) \times [0,T]$, to the set of points

$$(s,b,\tau) \in \Omega \times [0,T] \quad := \quad [0, s_{max}) \times [-b_{max}, b_{max}] \times [0,T], \tag{4.6}$$

where s_{max} and b_{max} are sufficiently large and positive. Let $s^* < s_{max}$ and $r_{max} = \max(r_b, r_\ell)$. Following Dang and Forsyth (2014), we introduce the following sub-computational domains:

$$\Omega_{s_0} = \{0\} \times [-b_{max}, b_{max}], \tag{4.7}$$

$$\Omega_{s^*} = (s^*, s_{max}] \times [-b_{max}, b_{max}], \tag{4.8}$$

$$\Omega_{b_{max}} = (0, s^*] \times \left[-b_{max} e^{r_{max}T}, -b_{max}\right) \cup \left(b_{max}, b_{max} e^{r_{max}T}\right], \tag{4.9}$$

$$\Omega_{\mathcal{B}} = \{(s,b) \in \Omega \setminus \Omega_{s^*} \setminus \Omega_{s_0} :\ W(s,b) \le 0\}, \tag{4.10}$$

$$\Omega_{in} = \Omega \setminus \Omega_{s^*} \setminus \Omega_{s_0} \setminus \Omega_{\mathcal{B}}. \tag{4.11}$$

Observe that $\Omega_{\mathcal{B}}$ is the localized insolvency region, Ω_{in} is the interior of the localized solvency region, while Ω_{s_0} is the boundary where $s = 0$. The buffer regions Ω_{s^*} and $\Omega_{b_{max}}$ ensure that the risky asset jumps and the risk-free asset interest payments, respectively, do not take us outside the computational grid (see d'Halluin et al. (2005) and Dang and Forsyth (2014)). Following the guidelines in d'Halluin et al. (2005), s^* and s_{max} are chosen to minimize the effect of the localization error for the jump terms. Operator $\mathcal{J}$ (4.3) is localized as

$$\mathcal{J}_\ell f(s,b,\tau) = \lambda \int_0^{s_{max}/s} f(\xi s, b, \tau) p(\xi) d\xi. \tag{4.12}$$

[9] The intervention operator plays a fundamental role in impulse control problems - see Oksendal and Sulem (2005).

Similar arguments as in Dang and Forsyth (2014) results in the following localized problem for V:

$$
\begin{aligned}
\min\left\{V_\tau - \mathcal{L}V - \mathcal{J}_\ell V + \rho\left(\sigma^2+\lambda\kappa_2\right)e^{2\mathcal{R}(b)\tau}s^2,\ \ V-\mathcal{M}V\right\} &= 0, \quad (s,b,\tau)\in\Omega_{in}\times(0,T],\\
\min\left\{V_\tau - \left(\sigma^2+2\mu+\lambda\kappa_2\right)V + \rho\left(\sigma^2+\lambda\kappa_2\right)e^{2\mathcal{R}(b)\tau}s^2,\ \ V-\mathcal{M}V\right\} &= 0, \quad (s,b,\tau)\in\Omega_{s^*}\times(0,T],\\
\min\left\{V_\tau - \mathcal{R}(b)\,bV_b,\ \ V-\mathcal{M}V\right\} &= 0, \quad (s,b,\tau)\in\Omega_{s_0}\times(0,T],\\
V(s,b,\tau) - V(0,W(s,b),\tau) &= 0, \quad (s,b,\tau)\in\Omega_{\mathcal{B}}\times(0,T],\\
V(s,b,\tau) - \frac{|b|}{b_{max}}V(s,\operatorname{sgn}(b)\,b_{max},\tau) &= 0, \quad (s,b,\tau)\in\Omega_{b_{max}}\times(0,T],\\
V(s,b,0) - W(s,b) &= 0 \quad (s,b)\in\Omega. \qquad (4.13)
\end{aligned}
$$

We briefly highlight certain aspects of the derivation of (4.13). Firstly, the localized problem in Ω_{s^*} is obtained as follows. Since the PIDE in the solvency region $\mathcal{N}$ (see (4.5)) has source term of $\mathcal{O}\left(s^2\right)$, it is reasonable to assume as in Wang and Forsyth (2012) that V has the asymptotic form $V(s\to\infty,b,\tau) = A_1(\tau)\,s^2$, for some function $A_1(\tau)$. Assuming that s^* in (4.8) is chosen sufficiently large so that this asymptotic form provides a reasonable approximation to V in Ω_{s^*}, substituting $V(s,b,\tau)\simeq A_1(\tau)\,s^2$ into the equation in (4.5) that holds for $(s,b,\tau)\in\mathcal{N}\times(0,T]$, leads to the corresponding equation that holds for $\Omega_{s^*}\times(0,T]$ in (4.13). Similar reasoning applies to the region $\Omega_{b_{max}}$, except that the initial condition of (4.5) gives $V(s,b\to\infty,\tau=0) = b$, which suggests the asymptotic form $V(s,|b|>|b_{max}|,\tau)\simeq A_2(\tau,s)\,b$ to be used in $\Omega_{b_{max}}$. Substituting $b=b_{max}$ and $b=-b_{max}$ allows for the solution in Ω to be used to approximate the solution in $\Omega_{b_{max}}$. The details of this approach can be found in Dang and Forsyth (2014).

Introducing the notation $\mathbf{x} = (s,b,\tau)$, $DV(\mathbf{x}) = (V_s, V_b, V_\tau)$ and $D^2V(\mathbf{x}) = V_{ss}$, the localized problem (4.13) for V can be written as the single equation

$$
FV \ \coloneqq\ F\left(\mathbf{x}, V(\mathbf{x}), DV(\mathbf{x}), D^2V(\mathbf{x}), \mathcal{M}V(\mathbf{x}), \mathcal{J}_\ell V(\mathbf{x})\right) = 0, \qquad (4.14)
$$

where the operator F is defined componentwise for each sub-computational domain so that all boundary conditions are included (see Dang and Forsyth (2014)). For example, if $\mathbf{x}\in\Omega_{in}\times(0,T]$,

$$
\begin{aligned}
FV = F_{in}V \ &\coloneqq\ F_{in}\left(\mathbf{x}, V(\mathbf{x}), DV(\mathbf{x}), D^2V(\mathbf{x}), \mathcal{M}V(\mathbf{x}), \mathcal{J}_\ell(\mathbf{x})\right), \qquad \text{if } \mathbf{x}\in\Omega_{in}\times(0,T] \quad (4.15)\\
&\coloneqq\ \min\left\{V_\tau - \mathcal{L}V - \mathcal{J}_\ell V + \rho\left(\sigma^2+\lambda\kappa_2\right)e^{2\mathcal{R}(b)\tau}s^2,\ \ V-\mathcal{M}V\right\}, \mathbf{x}\in\Omega_{in}\times(0,T].
\end{aligned}
$$

We observe that F satisfies the degenerate ellipticity condition (Jakobsen (2010)).

4.2 Discretization

To solve the localized problem (4.13) using finite differences, we use of (2.7) as the time grid, given in terms of τ as $\{\tau_n = T - t_{m+1-n} : n = 0,1,\ldots,m\}$, with $\Delta\tau = T/m = K_1\cdot h$, where $K_1>0$ is some constant independent of the discretization parameter h. We introduce nodes, which are not necessarily equally spaced, in the s-direction $\{s_i : i=1,\ldots,i_{max}\}$ and b-direction $\{b_j : j=1,\ldots,j_{max}\}$, where $\max_i(s_{i+1}-s_i) = K_2h$ and $\max_j(b_{j+1}-b_j) = K_3h$, with K_2 and K_3 positive and independent of h. Using the nodes in the b-direction, we define $\mathcal{Z}_h = \{b_j : j=1,\ldots,j_{max}\}\cap\mathcal{Z}$ to be the discretization of the admissible impulse space. The approximate solution of the value function at reference node (s_i,b_j,τ_n) is denoted by $V^n_{i,j} = V_h(s_i,b_j,\tau_n)$, where we use linear interpolation onto the computational grid if the spatial point required does not correspond to any grid point. We use the semi-Lagrangian timestepping scheme of Dang and Forsyth (2014) to handle the term $\mathcal{R}(b)\,bf_b$ in $\mathcal{L}f(s,b,\tau)$.

Following Forsyth and Labahn (2008); Wang and Forsyth (2008), the operator $\mathcal{P}$ is discretized as $\mathcal{P}_h$, ensuring that a positive coefficient discretization is obtained. The localized operator $\mathcal{J}_\ell$ (4.12) is discretized as $(\mathcal{J}_\ell)_h$ using the method described in d'Halluin et al. (2005), with quadrature weights

$\hat{w}_k^{i,j}$ at each (i,j)-node satisfying $0 \le \hat{w}_k^{i,j} \le 1$ and $\sum_k \hat{w}_k^{i,j} \le 1$. We also define the quantities $\widetilde{V}_{i,j}^n$, $q_{i,j}^n$ and $c_{i,j}$, calculated at node (s_i, b_j, τ_n), as

$$\widetilde{V}_{i,j}^n = \begin{cases} W(s_i, b_j), & n = 0, \\ \max\left[V_h\left(s_i, b_j e^{\mathcal{R}(b_j)\Delta\tau}, \tau_n\right), \max_{\eta \in \mathcal{Z}_h}\left\{V_h\left(S^+\left(s_i, b_j e^{\mathcal{R}(b_j)\Delta\tau}, \eta\right), \eta, \tau_n\right)\right\}\right], & n = 1, .., m, \end{cases} \tag{4.16}$$

$$q_{i,j}^n = \rho\left(\sigma^2 + \lambda\kappa_2\right) e^{2\mathcal{R}(b_j)\cdot\tau_n} s_i^2, \tag{4.17}$$

$$c_{i,j} = \frac{\rho\left(\sigma^2 + \lambda\kappa_2\right) e^{2\mathcal{R}(b_j)T}}{\left(\sigma^2 + 2\mu + \lambda\kappa_2 - 2\mathcal{R}(b_j)\right)} \cdot \left[1 - e^{\left(\sigma^2 + 2\mu + \lambda\kappa_2 - 2\mathcal{R}(b_j)\right)\Delta\tau}\right] s_i^2. \tag{4.18}$$

In Algorithm 4.1, we present the numerical scheme to solve problem $MQV_{t_n}(\rho)$, for a fixed $\rho > 0$, using fully implicit timestepping. The fixed point iteration method outlined in d'Halluin et al. (2005) is used to solve the discrete equations at each b-grid node and timestep, since it avoids a computationally expensive dense matrix solve resulting from jump terms (4.12). The derivation of the discretized equation (4.19) in Ω_{in} employs similar arguments as outlined in Dang and Forsyth (2014), while equation (4.20) is based on an analytical solution, over one timestep, of the PDE characterizing the continuation region in Ω_{s^*} (see (4.13)).

Algorithm 4.1 Numerical scheme to solve problem $MQV_{t_n}(\rho)$ for a fixed $\rho > 0$.

set $V_{i,j}^0 = W(s_i, b_j)$;
for $n = 1, \ldots, m$ do
  for $j = 1, \ldots, j_{max}$ do: Solve the following system of equations for $\left\{V_{i,j}^{n+1} : i = 1, \ldots, i_{max}\right\}$.

$$V_{i,j}^{n+1} - (\Delta\tau)\cdot\mathcal{P}_h V_{i,j}^{n+1} - (\Delta\tau)\cdot\left(\mathcal{J}_\ell\right)_h V_{i,j}^{n+1} + (\Delta\tau)\cdot q_{i,j}^{n+1} - \widetilde{V}_{i,j}^n = 0, \quad (s_i, b_j) \in \Omega_{in}, \tag{4.19}$$

$$V_{i,j}^{n+1} - \widetilde{V}_{i,j}^n \cdot e^{\left(\sigma^2 + 2\mu + \lambda\kappa_2\right)\Delta\tau} - c_{i,j} = 0, \quad (s_i, b_j) \in \Omega_{s^*}, \tag{4.20}$$

$$V_{i,j}^{n+1} - \widetilde{V}_{i,j}^n = 0, \quad (s_i, b_j) \in \Omega_{s_0}, \tag{4.21}$$

$$V_{i,j}^{n+1} - V_h\left(0, W\left(s_i, b_j e^{\mathcal{R}(b_j)\Delta t}\right), \tau_{n+1}\right) = 0, \quad (s_i, b_j) \in \Omega_{\mathcal{B}}, \tag{4.22}$$

$$V_{i,j}^{n+1} - |b_j|\cdot V_h\left(s_i, \mathrm{sgn}(b_j)\, b_{max}, \tau_{n+1}\right)/b_{max} = 0, \quad (s_i, b_j) \in \Omega_{b_{max}}. \tag{4.23}$$

  end for
end for

Remark 4.1. (Solution of auxiliary problems) The optimal control $\mathcal{C}_n^{q*}$ obtained from Algorithm 4.1 is used to solve two PIDEs (Oksendal and Sulem (2005)) for the two auxiliary functions $U^q(s, b, t_n)$ and $Q^q(s, b, t_n)$ required in constructing the MQV frontier (2.2). This is computationally inexpensive since the optimal control is known - see for example Wang and Forsyth (2012).

Remark 4.2. (Complexity) Using the same reasoning as in Dang and Forsyth (2014), it can be shown that the total complexity of constructing the MQV frontier (2.2) using Algorithm 4.1 is $\mathcal{O}\left(1/h^5\right)$, which is the same as the complexity of constructing a TCMV efficient frontier (Van Staden et al. (2018)).

4.3 Convergence to the viscosity solution

In general, since the solution of problems involving quasi-integrovariational inequalities such as (4.14) cannot be expected to be sufficiently smooth to admit a solution in the classical sense (Oksendal and Sulem (2005)), we seek a viscosity solution to (4.14). The convergence of the numerical solution of the numerical scheme (4.19)-(4.23) to the viscosity solution of (4.14) is established in the following theorem.

Theorem 4.3. *(Convergence) Assume that (4.14) satisfies a strong comparison property (see Dang and Forsyth (2014)) in $\Omega_{in} \cup \Gamma$, where $\Gamma \subseteq \partial\Omega_{in}$, with $\partial\Omega_{in}$ denoting the boundary of Ω_{in}. The numerical scheme (4.19)-(4.23) is consistent, monotone and ℓ_∞-stable. The numerical solution therefore converges to the unique, continuous viscosity solution of (4.14) in $\Omega_{in} \cup \Gamma$.*

Proof. If the consistency, monotonicity and ℓ_∞-stability of the numerical scheme (4.19)-(4.23) can be established, the conclusion follows from the results in Barles and Souganidis (1991). The local consistency of the scheme can be established as in Dang and Forsyth (2014), and this result is combined with the same steps as in Huang and Forsyth (2012) to conclude that the scheme (4.19)-(4.23) is consistent in the viscosity sense with equation (4.14). Proving the monotonicity and ℓ_∞-stability of the scheme can be done using the same steps as in Forsyth and Labahn (2008), which rely on the following properties of the proposed scheme: (i) fully implicit timestepping, together with (ii) the positive coefficient condition in the discretization of $\mathcal{P}$, (iii) the conditions on the quadrature weights in the discretization of $\mathcal{J}_\ell$, and (iv) the use of linear interpolation if necessary to obtain $V_h(\cdot)$. Finally, for a detailed discussion regarding the strong comparison assumption, see Dang and Forsyth (2014). □

Remark 4.4. (Discrete rebalancing) Up to this point, this section has only been concerned with rebalancing the portfolio at every timestep (continuous rebalancing). Algorithm 4.1 can be modified easily to handle discrete rebalancing. Specifically, multiple timesteps are introduced between any two rebalancing times τ_n and τ_{n+1}, where the discretized equations (4.19)-(4.23) are still solved, but at these additional timesteps only interest payments on the risk-free asset are made. This reduces the complexity of the algorithm (Remark 4.2) to $\mathcal{O}\left(1/h^4 \left|\log h\right|\right)$ for the construction of the MQV frontier.

5 Numerical results

5.1 Empirical data and calibration

In order to parameterize the underlying asset dynamics, the same calibration data and techniques are used as detailed in Dang and Forsyth (2016); Forsyth and Vetzal (2017). We briefly summarize the empirical data sources. The risky asset data is based on daily total return data (including dividends and other distributions) for the period 1926-2014 from the CRSP's VWD index[10], which is a capitalization-weighted index of all domestic stocks on major US exchanges. The risk-free rate is based on 3-month US T-bill rates[11] over the period 1934-2014, and has been augmented with the NBER's short-term government bond yield data[12] for 1926-1933 to incorporate the impact of the 1929 stock market crash. Prior to calculations, all time series were inflation-adjusted using data from the US Bureau of Labor Statistics[13].

In terms of calibration techniques, the calibration of the jump models is based on the thresholding technique of Cont and Mancini (2011); Cont and Tankov (2004) using the approach of Dang and Forsyth (2016); Forsyth and Vetzal (2017) which, in contrast to maximum likelihood estimation of jump model parameters, avoids problems such as ill-posedness and multiple local maxima[14]. In the

[10]Calculations were based on data from the Historical Indexes 2015©, Center for Research in Security Prices (CRSP), The University of Chicago Booth School of Business. Wharton Research Data Services was used in preparing this article. This service and the data available thereon constitute valuable intellectual property and trade secrets of WRDS and/or its third party suppliers.

[11]Data has been obtained from `See http://research.stlouisfed.org/fred2/series/TB3MS`.

[12]Obtained from the National Bureau of Economic Research (NBER) website, `http://www.nber.org/databases/macrohistory/contents/chapter13.html`.

[13]The annual average CPI-U index, which is based on inflation data for urban consumers, were used - see `http://www.bls.gov.cpi` .

[14]If $\Delta\hat{X}_i$ denotes the ith inflation-adjusted, detrended log return in the historical risky asset index time series, a jump is identified in period i if $\left|\Delta\hat{X}_i\right| > \alpha\hat{\sigma}\sqrt{\Delta t}$, where $\hat{\sigma}$ is an estimate of the diffusive volatility, Δt is the time period over

case of GBM, standard maximum likelihood techniques are used. The calibrated parameters are provided in Table 5.1.

Table 5.1: Calibrated risky and risk-free asset process parameters

	Models		
Parameters	GBM	Merton	Kou
μ (drift)	0.0816	0.0817	0.0874
σ (diffusive volatility)	0.1863	0.1453	0.1452
λ (jump intensity)	n/a	0.3483	0.3483
$\widetilde{m}$ (log jump multiplier mean)	n/a	-0.0700	n/a
$\widetilde{\gamma}$ (log jump multiplier stdev)	n/a	0.1924	n/a
ν (probability of up-jump)	n/a	n/a	0.2903
ζ_1 (exponential parameter up-jump)	n/a	n/a	4.7941
ζ_2 (exponential parameter down-jump)	n/a	n/a	5.4349
r (risk-free rate)	0.00623	0.00623	0.00623

5.2 Convergence analysis and validation

The convergence of the Algorithm 4.2 to the viscosity solution of the HJB quasi-integrovariational inequality (4.5) has been established in Theorem 4.3. The objective of this subsection is two-fold: (i) in the case of continuous rebalancing with no constraints, we confirm that the numerical solution converges to the analytical solution, and establish the rate of convergence, and (ii) use Monte Carlo simulation to verify the numerical results in cases where no analytical solutions are available.

5.2.1 Analytical solutions

Table 5.2 provides the timestep and grid information[15] for testing convergence of the numerical solution to the analytical solution (3.17)-(3.18). Table 5.3 summarizes the numerical convergence analysis for a

Table 5.2: Grid and timestep refinement levels for convergence analysis to analytical solution

Refinement level	Timesteps	s-grid nodes	b-grid nodes
0	30	71	140
1	60	1410	280
2	120	280	560
3	240	560	1120
4	480	1120	2240

scalarization parameter $\rho = 0.0026$, initial wealth $w_0 = 100$, maturity $T = 2$ years. While the results are only shown for the Merton model, qualitatively similar results are obtained in the case of the Kou and GBM models. The "Error" column gives the difference between the analytical solution[16] obtained using (3.17)-(3.18) and the numerical solution provided in the "PDE" column, while the "Ratio"

which the log return has been calculated, and α is a threshold parameter used to identify a jump. For both the Merton and Kou models, the parameters in Table 5.1 is based on a value of $\alpha = 3$, which means that a jump is only identified in the historical time series if the absolute value of the inflation-adjusted, detrended log return in that period exceeds 3 standard deviations of the "geometric Brownian motion change", definitely a highly unlikely event.

[15]Equal timesteps are used, while the grids in the s- and b-direction are not uniform.

[16]Due to the equivalence between the TCMV and MQV problems in the case of continuous rebalancing and no investment constraints, the analytical solution of $Qstd^{x_0,t=0}_{\mathcal{C}^{q*}}[W(T)]$, calculated according to (2.27), is also given by (3.18). This can be seen by simply re-arranging the resulting (identical) value functions.

column shows the ratio of successive errors with each increase in the refinement level. As expected, we observe first-order (or slightly faster) convergence of the numerical solution to the analytical solution as the mesh is refined.

Table 5.3: Convergence to the analytical solutions (see (3.17)-(3.18))

Ref. level	Expected value (Analytical soln.165.08)			Standard deviation (Analytical soln.110.00)			$Qstd^{x_0,t=0}_{\mathcal{C}^{q*}}[W(T)]$ (Analytical soln.110.00)		
	PDE soln.	Error	Ratio	PDE soln.	Error	Ratio	PDE soln.	Error	Ratio
0	165.47	0.39	-	110.40	0.40	-	114.49	4.49	-
1	165.24	0.16	2.43	110.15	0.15	2.69	111.60	1.60	2.81
2	165.14	0.07	2.46	110.06	0.06	2.52	110.62	0.62	2.58
3	165.10	0.03	2.57	110.03	0.03	2.28	110.25	0.25	2.43
4	165.09	0.01	2.50	110.01	0.01	2.33	110.11	0.11	2.28

5.2.2 Monte Carlo validation

Analytical solutions are not available for the MQV problem in the case where the portfolio is rebalanced monthly and liquidated in the event of insolvency, interest is settled daily on the risk-free asset, and maximum leverage constraints are applicable. For illustrative purposes, we assume the Kou model for the risky asset, initial wealth $w_0 = 100$, maturity $T = 2$ years, $\rho = 0.001$, and consider maximum leverage values of both $q_{\max} = 1.5$ and $q_{\max} = 1.0$. At each timestep of the numerical PDE solution, computed using 560 s-grid nodes, 1120 b-grid nodes, and 720 timesteps in total, we output and store the computed optimal strategy for each discrete state value. A total of 8 million Monte Carlo simulations for the portfolio are carried out from $t = 0$ to $t = T$, using the same investment parameters, with rebalancing occuring monthly in accordance with the stored PDE-computed optimal strategy for the corresponding rebalancing time[17]. Table 5.4 compares the results from the numerical method ("PDE" column) to the results calculated from the Monte Carlo simulation, illustrating that the values of the mean and standard deviation of terminal wealth, as well as $Qstd^{x_0,t=0}_{\mathcal{C}^{q*}}[W(T)]$, agree.

Table 5.4: Validating the numerical PDE solution using Monte Carlo simulation

Max. leverage	$E^{x_0,t=0}_{\mathcal{C}^{q*}}[W(T)]$		$Qstd^{x_0,t=0}_{\mathcal{C}^{q*}}[W(T)]$		$Stdev^{x_0,t=0}_{\mathcal{C}^{q*}}[W(T)]$	
	PDE	Simulation	PDE	Simulation	PDE	Simulation
$q_{\max} = 1.5$	129.10	129.08	57.79	57.87	65.21	65.25
$q_{\max} = 1.0$	119.11	119.11	35.93	35.97	39.16	38.81

5.3 MQV frontiers and MV efficient frontiers

In this subsection, we assess the impact of investment constraints and other assumptions on MQV frontiers, and compare the results with the corresponding TCMV efficient frontiers. Table 5.5 outlines the assumptions underlying five experiments specifically constructed to highlight the impact of different investment constraints. The interest rates and transaction costs used in Experiments 4 and 5 align to those used in Van Staden et al. (2018), while a leverage constraint of $q_{\max} = 1.0$, used for Experiments 3 and 5, implies that leverage is not allowed (see (2.14)).

All frontier results in this subsection assumes a maturity of $T = 20$ years, initial wealth $w_0 = 100$, and the annual rebalancing of the portfolio with approximately daily interest payments (364 per year)

[17] If required, interpolation is used to determine the optimal strategy for a given state value.

Table 5.5: Details of experiments

Experiment	Lending/ borrowing rates		If insolvent	Leverage constraint	Transaction costs	
	r_ℓ	r_b			Fixed (c_1)	Prop.(c_2)
Experiment 1	0.00623	0.00623	Continue trading	None	0	0
Experiment 2	0.00623	0.00623	Liquidate	$q_{\max} = 1.5$	0	0
Experiment 3	0.00623	0.00623	Liquidate	$q_{\max} = 1.0$	0	0
Experiment 4	0.00400	0.06100	Liquidate	$q_{\max} = 1.5$	0.001	0.005
Experiment 5	0.00400	0.06100	Liquidate	$q_{\max} = 1.0$	0.001	0.005

on the risk-free asset. To ensure the accuracy of the results, each point on a frontier is constructed using a very fine grid, namely 7,280 equal timesteps, together with 1,105 b-grid and 561 s-grid nodes, respectively.

5.3.1 Model choice

The impact of model choice on the MQV frontier is illustrated in Figure 5.1. Since the assumption of daily interest payments used for the construction of frontiers in this section approximates the continuous compounding of interest with reasonable accuracy, the investment constraints of Experiment 1 aligns closely with Assumption 3.1.

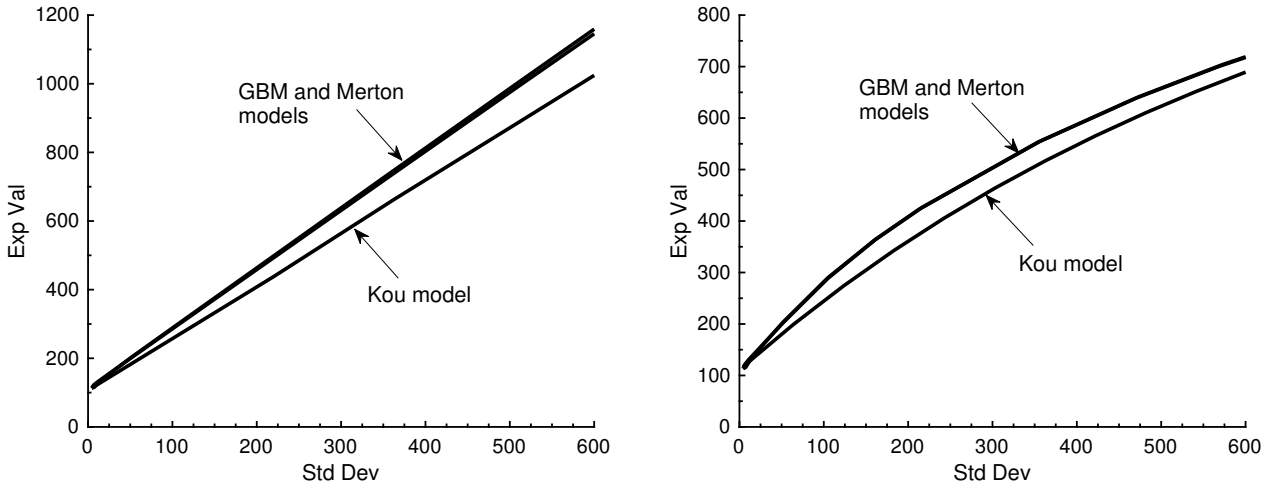

(a) Experiment 1 - No constraints

(b) Experiment 2 - With liquidation and leverage constraint ($q_{\max} = 1.5$)

Figure 5.1: MQV frontiers: Effect of model choice (GBM, Merton, Kou models).

The differences in Figure 5.1 (a) can therefore be explained by referencing the slope of the frontiers reported in Theorem 3.6, in conjuction with the model parameters in Table 5.1. We observe that all models have similar μ values. Furthermore, the combination of parameters $\left(\sigma^2 + \lambda\kappa_2\right)$ for the Merton model and σ^2 for the GBM model are closely aligned, in other words, the higher diffusive volatility of the GBM model has a similar effect as incorporating jumps using the Merton model, resulting in roughly equal MQV frontier slope values calculated using (3.10). Since the jump multiplier has a significantly higher variance for the Kou model as compared to the Merton model, when calibrated to the same data, the resulting higher κ_2 value for the Kou model[18] decreases the slope (3.10) of the associated MQV frontier. As seen in Figure 5.1 (b), even when investment constraints are present,

[18]For the Kou model, $\kappa_2 = \mathbb{E}\left[(\xi - 1)^2\right] \simeq 0.084$, compared to the Merton model where $\kappa_2 = 0.036$.

the MQV frontiers of the GBM and Merton models remain effectively indistinguishable, and above the frontier based on the Kou model. Qualitatively similar results also hold for the other experiments, and are therefore omitted.

5.3.2 Investment constraints

Figure 5.2 illustrates the effect of investment constraints on the MQV frontiers for the GBM and Kou models (qualitatively similar results are obtained for the Merton model). Regardless of model choice, we observe that introducing just two basic constraints, namely liquidation in the event of insolvency and a maximum leverage constraint (Experiment 2), has a significant impact on the MQV frontier. If we additionally introduce more realistic interest rates and transaction costs (Experiment 4), the expected terminal wealth that can be achieved is further reduced, especially for higher levels of risk. This follows from the observation that a higher standard deviation of terminal wealth is achieved only by increasing the investment in the risky asset, a strategy which is executed by borrowing to invest. Since the borrowing costs are substantially higher and transaction costs are not zero in Experiment 4, the expected value of the terminal wealth is reduced compared to Experiment 2 for any given value of the standard deviation.

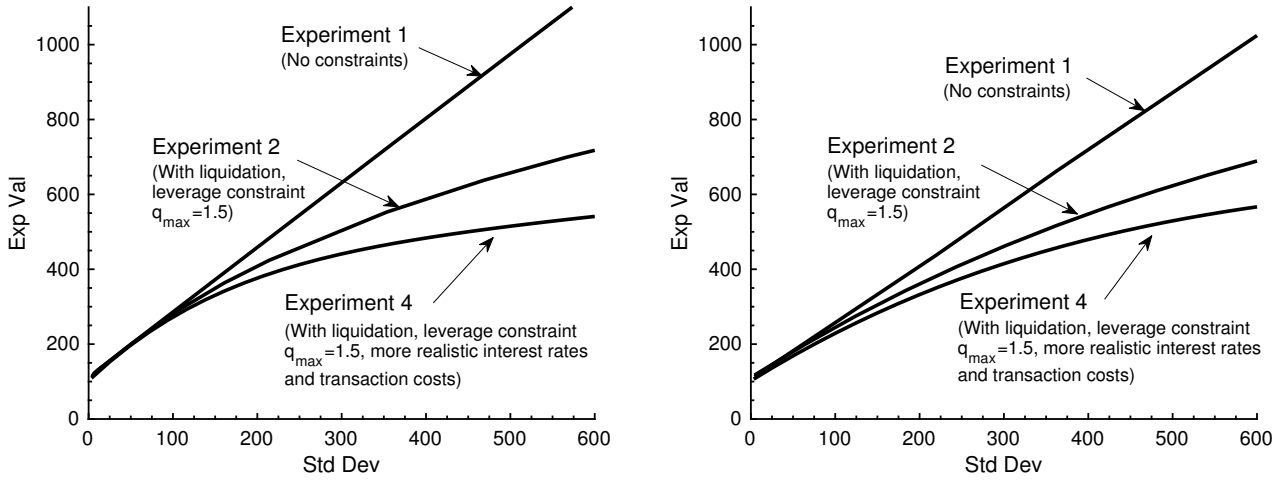

(a) GBM model

(b) Kou model

Figure 5.2: MQV frontiers: Relative effect of investment constraints (GBM and Kou model).

Figure 5.3 investigates the role of the maximum leverage ratio on the MQV frontiers. Recall from (2.14) that a value of $q_{\max} = 1.0$ means leverage is not allowed, which is common in the case of many pension fund investments. In Figure 5.3 (a) we observe that, for any given standard deviation of terminal wealth, a strategy constrained by liquidation in the event of bankruptcy and $q_{\max} = 1.5$ (Experiment 2) is expected to significantly outperform a strategy subject to otherwise similar constraints except that no leverage is allowed (Experiment 3). However, once more realistic interest rates and transaction costs are introduced, Figure 5.3 (b) shows that this difference largely disappears. The reason is that in Experiments 4 and 5, the cost of borrowing to invest is substantially higher than in the case of Experiments 2 and 3, thereby significantly increasing the cost of any strategy relying on leverage. The results of Experiments 4 and 5 (Figure 5.3 (b)) are therefore much less sensitive to the maximum leverage ratio allowed.

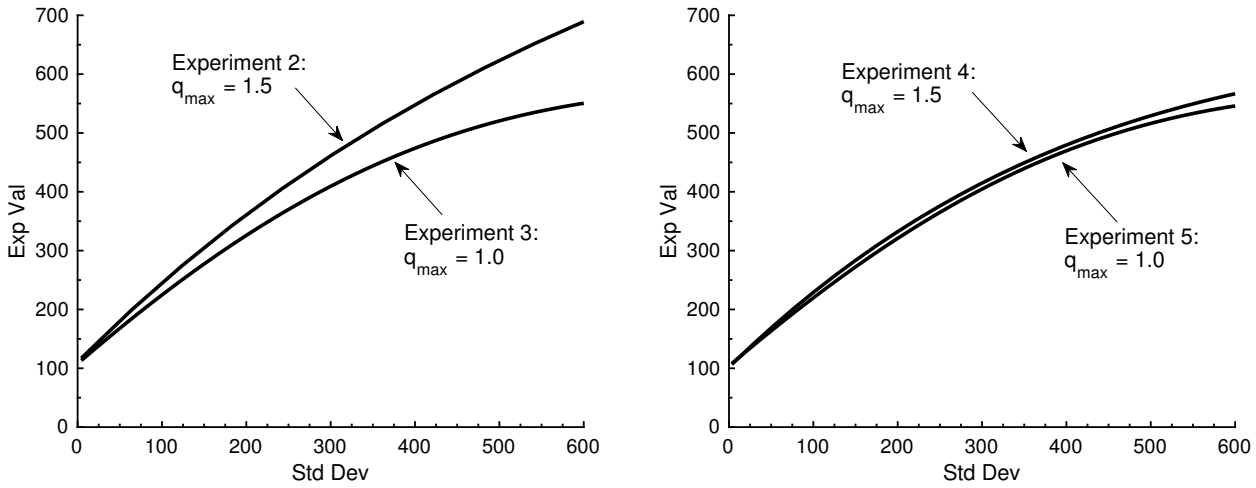

(a) Kou model, Experiments 2 and 3

(b) Kou model, Experiments 4 and 5

Figure 5.3: MQV frontiers: Effect of reducing the maximum leverage ratio, $q_{\max}$ (Kou model).

5.3.3 Comparison of frontiers

In this subsection, we compare MQV frontiers with TCMV and Pre-commitment MV efficient frontiers[19] based on otherwise identical assumptions, parameters and investment constraints. Results are illustrated for the Kou model only, since other models yield qualitatively similar results.

Figure 5.4 (a) shows that the MQV frontier and TCMV efficient frontier is indistinguishable in the case of Experiment 1. Based on Theorem 3.6, this is to be expected, since the details of Assumption 3.1 are largely the same as the assumptions of Experiment 1 in combination with the use of daily interest payments in the semi-Lagrangian timestepping scheme, which approximates continuous compounding. The Pre-commitment MV efficient frontier lies above the TCMV efficient frontier, since the TCMV problem, while having the same objective function, is subject to the additional time-consistency constraint. This remains the case even when investment constraints are introduced (Figure 5.4 (b)), although the difference between the efficient frontiers is substantially reduced.

More importantly, we observe that the MQV strategy is more MV efficient than the associated TCMV strategy, in that the MQV frontier is either indistinguishable from, or slightly above, the corresponding TCMV efficient frontier. This has also been observed in the case of no jumps and continuous rebalancing (Wang and Forsyth (2012)). In the present setting of jumps in the risky asset process and discrete rebalancing, we note that this observation remains true regardless of the investment constraints introduced, such as if liquidation in the event of insolvency and a maximum leverage constraint is introduced (Figure 5.4 (b)), if leverage is not allowed (Figure 5.5 (a)), as well as if more realistic interest rates and transaction costs are implemented (Figure 5.5 (b)). The reasons for this are explored in more detail in the subsequent sections.

5.4 Comparing terminal wealth distributions

A potential drawback from making conclusions based only on the frontiers presented above (Subsection 5.3.3), is that such conclusions necessarily only consider the relation between the standard deviation and expected value of terminal wealth. From the perspective of an investor, however, the overall distribution of terminal wealth might be just as important.

To compare terminal wealth distributions for the MQV and TCMV strategies, we fix the standard deviation of terminal wealth under the respective optimal strategies at a value of 400. This corresponds

[19] Pre-commitment MV and TCMV efficient frontiers are constructed using the techniques outlined in Dang and Forsyth (2014) and Van Staden et al. (2018), respectively.

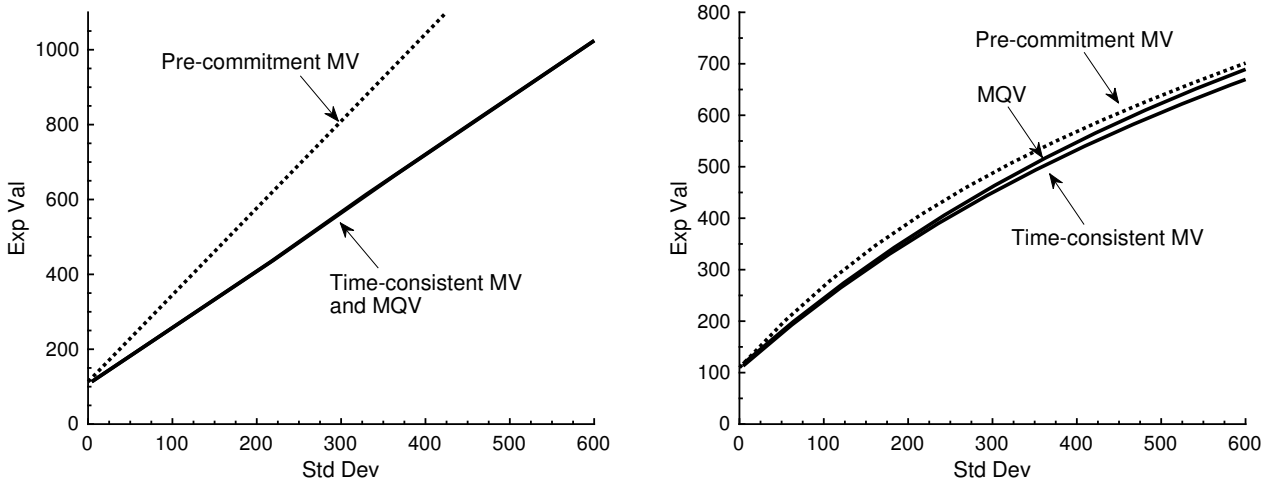

(a) Experiment 1 (b) Experiment 2

Figure 5.4: MQV frontiers vs. TCMV and Pre-commitment MV efficient frontiers, Experiments 1 and 2 (Kou model).

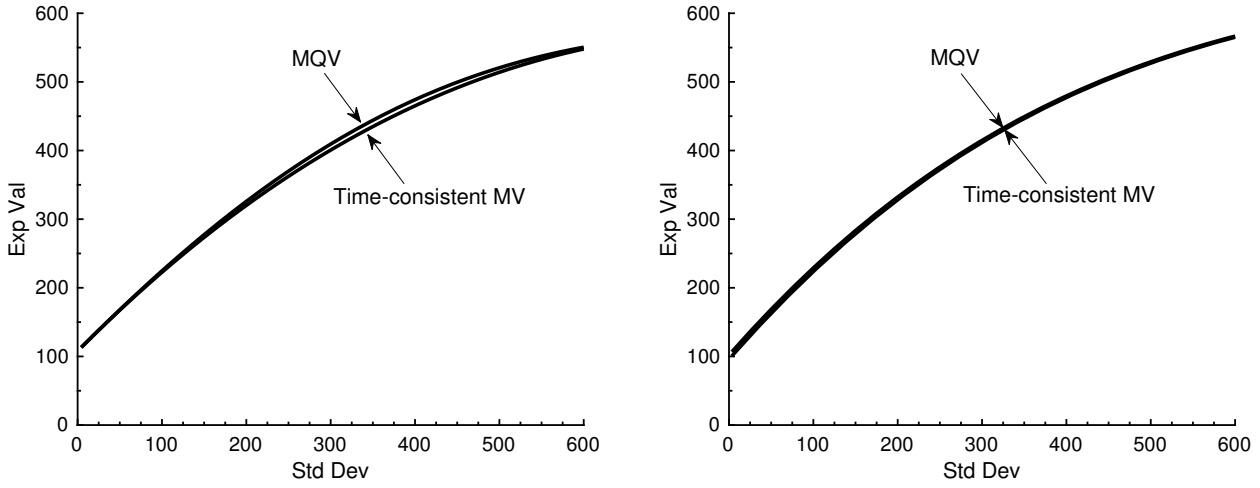

(a) Experiment 3 (b) Experiment 4

Figure 5.5: MQV frontiers vs. TCMV efficient frontiers, Experiments 3 and 4 (Kou model).

to fixing a value of 400 on the x-axis in Figures 5.4 and 5.5. When solving the MQV and TCMV problems corresponding to these points on the frontiers, at each timestep of the algorithm, we output and store the computed optimal strategy for each discrete state value. We then carry out 10 million Monte Carlo simulations for the portfolio from $t = 0$ to $t = T$ using investment parameters identical to those used in the numerical PDE solution, and rebalance the portfolio in accordance with the stored PDE-computed optimal strategy at each rebalancing time. For each simulation, the resulting terminal wealth $W(T)$ value is stored.

Figure 5.6 shows a comparison of the simulated distribution of terminal wealth $W(T)$ for Experiments 3 and 4 under the MQV and TCMV optimal strategies achieving a standard deviation of $W(T)$ equal to 400. Note that Experiments 2 and 5 yield qualitatively similar results, so these distributions are not shown. In addition, Table 5.6 summarizes selected percentiles from the simulated distributions obtained for Experiments 2, 3, 4 and 5.

Based on Figure 5.6 and Table 5.6, we conclude the following. The MQV and TCMV distributions of terminal wealth are generally very similar, even in the presence of investment constraints. However, in all experiments, for the same standard deviation of terminal wealth, the 25th percentile, median and

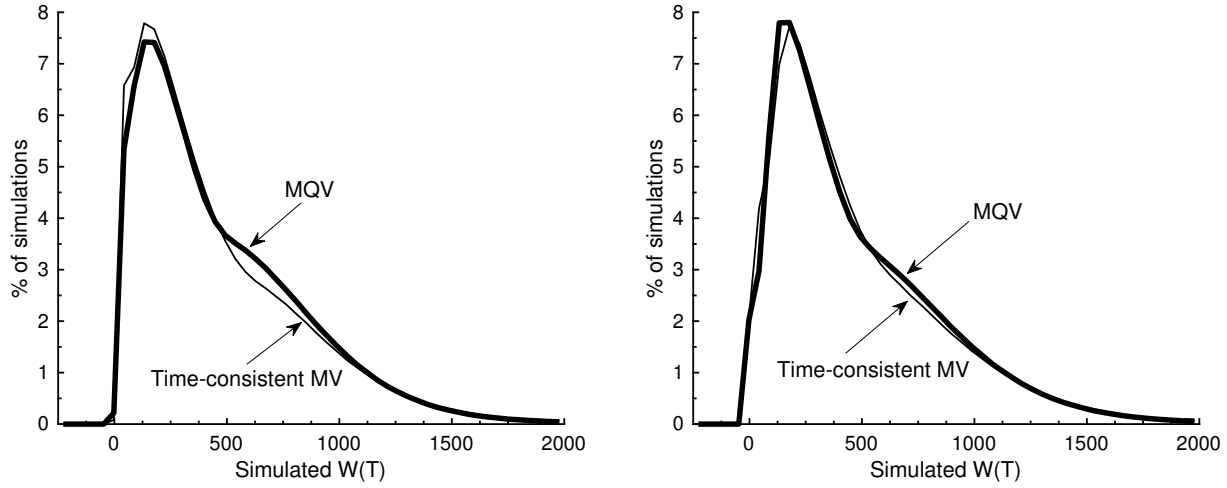

(a) Experiment 3

(b) Experiment 4

Figure 5.6: Simulated distribution of terminal wealth $W(T)$ under the MQV-optimal and TCMV optimal strategy, standard deviation equal to 400, Experiments 3 and 4 (Kou model).

Table 5.6: Experiments 2, 3, 4 and 5: Selected percentiles (rounded to nearest integer) from the simulated distribution of the terminal wealth under the MQV-optimal and TCMV-optimal strategy. In each case, a standard deviation of terminal wealth equal to 400 is obtained.

Percentile	Experiment 2		Experiment 3		Experiment 4		Experiment 5	
	MQV	TCMV	MQV	TCMV	MQV	TCMV	MQV	TCMV
5th	18	36	61	49	65	52	59	44
10th	58	83	97	88	106	100	95	86
25th	224	218	188	177	193	194	186	174
50th	521	480	374	350	372	368	370	340
75th	794	762	685	662	687	675	677	630
90th	1053	1049	986	991	1007	1018	980	972
95th	1226	1248	1183	1207	1216	1247	1178	1200

75th percentile of the wealth distribution achieved by the MQV strategy exceeds that of the TCMV strategy. Furthermore, in Experiments 4 and 5, where more realistic interest rates and transaction costs are applied in addition to leverage constraints and liquidation in the case of insolvency, the MQV strategy results in improved downside outcomes (5th and 10th percentiles in Table 5.6), while only slightly underperforming the TCMV strategy in terms of the extreme upside (95th percentile).

5.5 Comparison of optimal strategies

An investor facing a choice between an MQV and TCMV strategy might reasonably observe that the terminal wealth outcomes are very similar, but perhaps slightly in favor of the MQV strategy. However, many investors, for example institutional investors such as pension funds, have a keen interest in how the risk exposure of an investment strategy evolves over time.

To compare the optimal investment strategy according to the MQV and TCMV approaches, we perform the same Monte Carlo simulation as described in Subsection 5.4 used in the construction of Table 5.6. As in that case, we solve the MQV and TCMV problems corresponding to a standard deviation of terminal wealth equal to 400, output and store the computed optimal strategy for each discrete state value, and rebalance the portfolio according to the stored strategies in a Monte Carlo simulation of the portfolio. However, instead of limiting our attention to just the terminal wealth

obtained from each simulation, we consider the fraction of wealth invested in the risky asset at each point in time in each simulation. In this way, a distribution of the fraction of wealth invested in the risky asset at each point in time, required by each strategy, can be constructed.

Figure 5.7 shows the median (50th percentile), as well as the 25th and 75th percentiles, of the distribution of the fraction of wealth invested in the risky asset according to the MQV-optimal strategy and the TCMV-optimal strategy. The results are only shown for the Kou model and Experiment 2, with qualitatively similar results obtained for other models and experiments, with the exception of Experiment 1, where the two strategies are effectively identical[20].

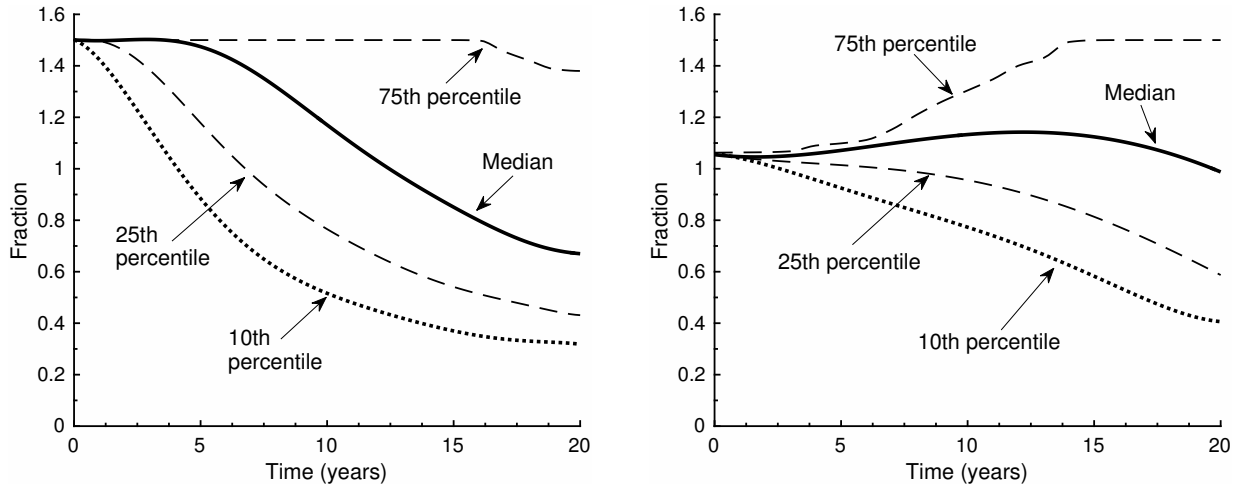

(a) MQV-optimal strategy

(b) TCMV-optimal strategy

Figure 5.7: MQV-optimal and TCMV-optimal fraction of wealth invested in the risky asset over time, Experiment 2 (Kou model). Standard deviation of terminal wealth equal to 400.

Comparing Figure 5.7 (a) and Figure 5.7 (b), we observe that the MQV-optimal strategy calls for a significantly higher investment in the risky asset (effectively the maximum investment possible, given a leverage constraint of $q_{\max} = 1.5$ in Experiment 2) during the early stages of the investment period. However, as time passes, the MQV strategy calls for a reduction in risky asset exposure, so that the MQV-optimal median fraction of wealth invested in the risky asset drops below, and remains below, the corresponding median fraction for the TCMV-optimal strategy from just after the middle of the investment time horizon until maturity (i.e. after about 10 years). In the case of the 10th percentile, this effect is even more dramatic, with the MQV-optimal fraction of wealth invested in the risky asset dropping below the TCMV-optimal fraction after only about 5 years.

Intuitively, the results of Figure 5.7 can be explained as follows. The TCMV investor is only concerned with terminal wealth, and acts consistently with mean-variance risk preferences throughout the investment time horizon (see for example Cong and Oosterlee (2016)). In contrast, the MQV investor is concerned with the expected value of the (future-valued) QV of wealth accumulated over the investment time horizon. For smaller wealth values, the presence of a leverage constraint implies that the amount invested in the risky asset is necessarily also smaller, which reduces the expected value of the QV of wealth (see for example equation (A.2) in Appendix A). For a fixed level of $\rho > 0$, the MQV investor therefore places a relatively larger weight on maximizing the expected value of terminal wealth if current wealth levels are low, which results in a larger MQV-optimal fraction of wealth required to be invested in the risky asset. However, as time passes and wealth increases, maintaining the same fraction of wealth in the risky asset requires ever larger amounts invested in the risky asset, a strategy which is costly in terms of QV. The MQV-optimal strategy therefore calls for a fairly rapid reduction in exposure to the risky asset over time if past returns are favorable, in contrast with the

[20]Based on the results in Section 3, the similarity between strategies in the case of Experiment 1 is to be expected.

TCMV strategy.

A more rigorous explanation of the observed differences in optimal strategies follows from a direct comparison of the optimal controls used in the Monte Carlo simulation to generate Figure 5.7. To this end, Figure 5.8 presents the heatmaps of the MQV and TCMV optimal control (in terms of the fraction of wealth invested in the risky asset) as a function of time and wealth. Compared to the TCMV strategy, the MQV strategy calls for a faster reduction in risky asset exposure as wealth increases, while for a given level of wealth, the MQV optimal fraction of wealth invested in the risky asset is fairly stable over time.

Considering the particular case of an initial wealth of $w_0 = 100$ used for constructing the frontiers in Subsection 5.3.3 and Figure 5.7, the MQV optimal strategy calls for the maximum possible investment in the risky asset given the leverage constraint, in contrast to the TCMV optimal strategy, which requires a much lower investment. If returns are favourable, so that wealth grows sufficiently over time, the MQV optimal control calls for significantly larger reduction in the investment in the risky asset compared to the TCMV optimal control. Finally, we observe that both of these strategies are contrarian in the sense that, all else being equal, the investment in the risky asset is increased if past returns have been unfavourable.

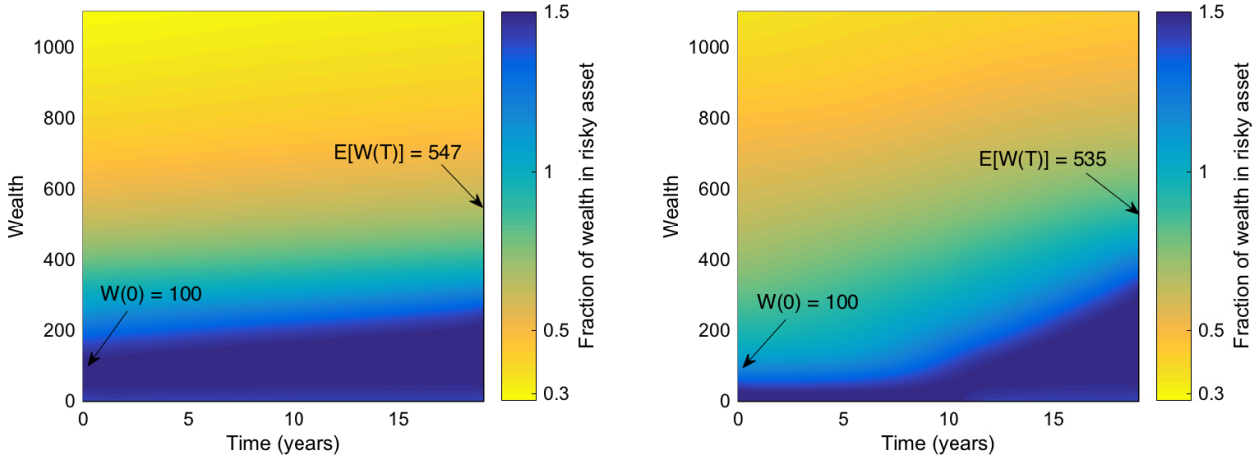

(a) MQV-optimal strategy

(b) TCMV-optimal strategy

Figure 5.8: Optimal control expressed as a fraction of wealth in the risky asset, Experiment 2 (Kou model). Standard deviation of terminal wealth equal to 400.

6 Conclusions

In this paper, we investigate the relationship between the TCMV and MQV portfolio optimization problems and derive analytical solutions for the case of jumps in the risky asset process and discrete rebalancing of the portfolio, which leads to the following conclusions. Firstly, both problems result in identical trade-offs regarding the mean and variance of terminal wealth, so that an MV investor would be indifferent as to which objective is used. Secondly, for a fixed level of risk aversion the MQV-optimal strategy would call for a larger investment in the risky asset compared to the TCMV-optimal strategy. Thirdly, an alternative QV risk measure can be constructed to ensure the exact equivalence between the problems under more general conditions than those currently known in literature.

Furthermore, a numerical scheme together with a convergence proof is presented, enabling the solution of the MQV problem in the case where analytical solutions are not known. Under realistic investment constraints, the MQV and TCMV optimal terminal wealth distributions and investment strategies are compared and contrasted. We conclude that the MQV investor achieves essentially the same terminal wealth outcomes as the TCMV investor, but with an improved risk profile, since the

MQV strategy calls for a reduction in risky asset exposure over time. The MQV approach might therefore be especially attractive for investors wishing to obtain TCMV outcomes, but requiring more certainty regarding the portfolio value as some target date is approached. MQV optimization is therefore a potentially desirable alternative to TCMV optimization, particularly for long-term, institutional investors who may find the resulting risk profile more attractive.

We leave further analysis of the relationship between TCMV and MQV strategies, including the construction of alternative QV risk measures ensuring the equivalence of these problems in even more general settings, for our future work.

Appendix A: Proof of Lemma 3.4 and Lemma 3.5

We give a proof of Lemma 3.4 and Lemma 3.5 that relies on backward induction. Consider a fixed set of rebalancing times $\mathcal{T}_m$ as in (2.7), and assume that Assumption 3.1 holds.

Suppose the system is in state $x = (s, b)$ at time t_n^-, where $t_n \in \mathcal{T}_m$. Since there is no intervention over the time interval $\left[t_n^+, t_{n+1}^-\right]$, the underlying dynamics (2.1) and (2.4) imply that $E_{\eta_n}^{x,t_n}\left[B\left(t_{n+1}^-\right)\right] = \eta_n e^{r\Delta t}$, and $Var_{\eta_n}^{x,t_n}\left[B\left(t_{n+1}^-\right)\right] = 0$, while $E_{\eta_n}^{x,t_n}\left[S\left(t_{n+1}^-\right)\right] = (s+b-\eta_n)\, e^{\mu\Delta t}$, and

$$Var_{\eta_n}^{x,t_n}\left[S\left(t_{n+1}^-\right)\right] = (s+b-\eta_n)^2\left(e^{\left(2\mu+\sigma^2+\lambda\kappa_2\right)\Delta t} - e^{2\mu\Delta t}\right), \tag{A.1}$$

$$E_{\eta_n}^{x,t_n}\left[\int_{t_n}^{t_{n+1}^-} e^{2r(T-t)} d\left\langle W\right\rangle_t\right] = (s+b-\eta_n)^2 e^{2r(T-t_n)}\frac{\left(e^{\mu\Delta t} - e^{r\Delta t}\right)}{K^q}, \tag{A.2}$$

Firstly, note that at maturity $t_{m+1} = T$, the value functions are trivially given by (3.1) and (3.5). Assume that the results of Lemma 3.4 and Lemma 3.5 hold for rebalancing time $t_{n+1} \in \mathcal{T}_m$, and fix an arbitrary state $x = (s, b)$ at time t_n^-. Let $X_{n+1} \coloneqq \left(S\left(t_{n+1}^-\right), B\left(t_{n+1}^-\right)\right)$.

Recalling the formulation of problem $TCMV_{t_n}(\rho)$ as (2.19), we have to maximize objective function $J^c(\eta_n; s, b, t_n)$, given by (2.20), over $\eta_n \in \mathbb{R}$. Using the result (A.1) together with the assumption that Lemma 3.4 holds at time t_{n+1}, we obtain $J^c(\eta_n; s, b, t_n)$ as the following quadratic function of η_n,

$$\begin{aligned} J^c(\eta_n; s, b, t_n) &= (s+b)\, e^{r(T-t_n)} e^{(\mu-r)\Delta t} - \rho\left[(s+b)^2 + \eta_n^2\right]\frac{\left(e^{\mu\Delta t} - e^{r\Delta t}\right) e^{2r(T-t_n)}}{e^{2r\Delta t} K^c} \\ &+ \left(e^{\mu\Delta t} - e^{r\Delta t}\right)\left[\left(\frac{T-t_n}{\Delta t} - 1\right)\left(\frac{1}{4\rho}K^c\right) + \eta_n\left(\frac{2\rho\,(s+b)\, e^{r(T-t_n)}}{e^{2r\Delta t}K^c} - \frac{1}{e^{r\Delta t}}\right) e^{r(T-t_n)}\right]. \end{aligned} \tag{A.3}$$

The value of η_n^{c*} maximizing (A.3), obtained from the first order condition, is given by (3.4). The value function (3.1) is given by $J^c(\eta_n^{c*}; s, b, t_n)$, while the auxiliary function (3.3) can be obtained in a similar way.

In the case of problem $MQV_{t_n}(\rho)$, the assumption that Lemma 3.5 holds at time t_{n+1}, together with (2.28) and (A.2), gives the objective function $J^q(\eta_n; s, b, t_n)$ (see (2.28)) to be maximized as the following quadratic function of η_n,

$$\begin{aligned} J^q(\eta_n; s, b, t_n) &= (s+b)\, e^{r(T-t_n)} e^{(\mu-r)\Delta t} - \rho\left[(s+b)^2 + \eta_n^2\right]\frac{\left(e^{\mu\Delta t} - e^{r\Delta t}\right) e^{2r(T-t_n)}}{K^q} \\ &+ \left(e^{\mu\Delta t} - e^{r\Delta t}\right)\left[\left(\frac{T-t_n}{\Delta t} - 1\right)\left(\frac{1}{4\rho}\frac{K^q}{e^{2r\Delta t}}\right) + \eta_n\left(\frac{2\rho\,(s+b)\, e^{r(T-t_n)}}{K^q} - \frac{1}{e^{r\Delta t}}\right) e^{r(T-t_n)}\right] \end{aligned} \tag{A.4}$$

From the first order condition, the value η_n^{q*} maximizing (A.4) is given by (3.9). After substitution and simplification, the value function (3.5) is obtained as $J^q\left(\eta_n^{q*}; s, b, t_n\right)$. The auxiliary functions (3.7) and (3.8) can be derived using similar arguments as in the derivation of (A.4).

The results of Lemma 3.4 and Lemma 3.5 therefore hold by backward induction.

References

Alia, I., F. Chighoub, and A. Sohail (2016). A characterization of equilibrium strategies in continuous-time mean–variance problems for insurers. *Insurance: Mathematics and Economics* (68), 212–223.

Almgren, R. and N. Chriss (2001). Optimal execution of portfolio transactions. *Journal of Risk* (3), 5–40.

Applebaum, D. (2004). *Lévy processes and stochastic calculus*. Cambridge University Press.

Barles, G. and P. Souganidis (1991). Convergence of approximation schemes for fully nonlinear second order equations. *Asymptotic Analysis* 4(3), 271–283.

Basak, S. and G. Chabakauri (2010). Dynamic mean-variance asset allocation. *Review of Financial Studies* 23, 2970–3016.

Bensoussan, A., K. C. Wong, S. C. P. Yam, and S. P. Yung (2014). Time-consistent portfolio selection under short-selling prohibition: From discrete to continuous setting. *SIAM Journal on Financial Mathematics* 5, 153–190.

Bjork, T., M. Khapko, and A. Murgoci (2017). On time-inconsistent stochastic control in continuous time. *Finance and Stochastics* 21, 331–360.

Bjork, T. and A. Murgoci (2010). A general theory of Markovian time inconsistent stochastic control problems. *Working paper* Available at http://ssrn.com/abstract=1694759.

Bjork, T. and A. Murgoci (2014). A theory of Markovian time-inconsistent stochastic control in discrete time. *Finance and Stochastics* (18), 545–592.

Brugiere, P. (1996). Optimal portfolio and optimal trading in a dynamic continuous time framework. *Nurenberg, Germany* 6'th AFIR Colloquium.

Cong, F. and C. Oosterlee (2016). On pre-commitment aspects of a time-consistent strategy for a mean-variance investor. *Journal of Economic Dynamics and Control* 70, 178–193.

Cont, R. and C. Mancini (2011). Nonparametric tests for pathwise properties of semi-martingales. *Bernoulli* (17), 781–813.

Cont, R. and P. Tankov (2004). *Financial modelling with jump processes*. Chapman and Hall / CRC Press.

Crandall, M., H. Ishii, and P. Lions (1992). User's guide to viscosity solutions of second order partial differential equations. *Bulletin of the American Mathematical Society* 27(1), 1–67.

Cui, X., L. Xu, and Y. Zeng (2015). Continuous time mean-variance portfolio optimization with piecewise state-dependent risk aversion. *Optimization Letters (Springer)* pp. 1–11.

Dang, D. and P. Forsyth (2014). Continuous time mean-variance optimal portfolio allocation under jump diffusion: A numerical impulse control approach. *Numerical Methods for Partial Differential Equations* 30, 664–698.

Dang, D. and P. Forsyth (2016). Better than pre-commitment mean-variance portfolio allocation strategies: A semi-self-financing Hamilton–Jacobi–Bellman equation approach. *European Journal of Operational Research* (250), 827–841.

d'Halluin, Y., P. Forsyth, and K. Vetzal (2005). Robust numerical methods for contingent claims under jump diffusion processes. *IMA Journal of Numerical Analysis* (25), 87–112.

Elton, E., M. Gruber, S. Brown, and W. Goetzmann (2014). *Modern portfolio theory and investment analysis*. Wiley, 9th edition.

Forsyth, P., J. Kennedy, S. Tse, and H. Windcliff (2012). Optimal trade execution: A mean quadratic variation approach. *Journal of Economic Dynamics and Control* 36, 1971–1991.

Forsyth, P. and G. Labahn (2008). Numerical methods for controlled Hamilton–Jacobi–Bellman PDEs in finance. *Journal of Compuational Finance* (11 (Winter)), 1–44.

Forsyth, P. and K. Vetzal (2017). Dynamic mean variance asset allocation: Tests for robustness. *International Journal of Financial Engineering* 4:2. 1750021 (electronic).

Hu, Y., H. Jin, and X. Zhou (2012). Time-inconsistent stochastic linear-quadratic control. *SIAM Journal on Control and Optimization* 50(3), 1548–1572.

Huang, Y. and P. Forsyth (2012). Analysis of a penalty method for pricing a guaranteed minimum withdrawal benefit (gmwb). *IMA Journal of Numerical Analysis* (32), 320–351.

Jakobsen, E. (2010). *Monotone schemes*. Encyclopedia of quantitative finance. Wiley, New York.

Kou, S. (2002). A jump-diffusion model for option pricing. *Management Science* 48(8), 1086–1101.

Li, D. and W.-L. Ng (2000). Optimal dynamic portfolio selection: multi period mean variance formulation. *Mathematical Finance* 10, 387–406.

Ma, K. and P. Forsyth (2016). Numerical solution of the Hamilton-Jacobi-Bellman formulation for continuous time mean variance asset allocation under stochastic volatility. *Journal of Computational Finance* 20:1, 1–37.

McNeil, A., R. Frey, and P. Embrechts (2015). *Quantitative Risk Management: Concepts, techniques and tools.* Princeton University Press.

Merton, R. (1976). Option pricing when underlying stock returns are discontinuous. *Journal of Financial Economics* 3, 125–144.

Oksendal, B. and A. Sulem (2005). *Applied Stochastic Control of Jump Diffusions.* Springer.

Rockafellar, R. and S. Uryasev (2002). Conditional value-at-risk for general loss distributions. *Journal of Banking and Finance* (26), 1443–1471.

Tse, S., P. Forsyth, J. Kennedy, and H. Windcliff (2013). Comparison between the mean-variance optimal and the mean-quadratic-variation optimal trading strategies. *Applied Mathematical Finance* 20(5), 415–449.

Van Staden, P. M., D. Dang, and P. Forsyth (2018). Time-consistent mean-variance portfolio optimization: a numerical impulse control approach. *Insurance: Mathematics and Economics* (83C), 9–28.

Vigna, E. (2016). On time consistency for mean-variance portfolio selection. *Working paper, Collegio Carlo Alberto* (476).

Wang, J. and P. Forsyth (2008). Maximal use of central differencing for Hamilton–Jacobi–Bellman PDEs in finance. *SIAM Journal on Numerical Analysis* (46), 1580–1601.

Wang, J. and P. Forsyth (2011). Continuous time mean variance asset allocation: A time-consistent strategy. *European Journal of Operational Research* (209), 184–201.

Wang, J. and P. Forsyth (2012). Comparison of mean variance like strategies for optimal asset allocation problems. *International Journal of Theoretical and Applied Finance* 15(2).

Zeng, Y. and Z. Li (2011). Optimal time-consistent investment and reinsurance policies for mean-variance insurers. *Insurance: Mathematics and Economics* 49(1), 145–154.

Zeng, Y., Z. Li, and Y. Lai (2013). Time-consistent investment and reinsurance strategies for mean–variance insurers with jumps. *Insurance: Mathematics and Economics* 52, 498–507.

Zhou, X. and D. Li (2000). Continuous time mean variance portfolio selection: a stochastic LQ framework. *Applied Mathematics and Optimization* 42, 19–33.